Korea Polymer Journal

Volume 6, Number 1 March 31, 1998

Statistical Thermodynamics of Semi-rigid Polymer Systems

Michael Hess

Department of Physical Chemistry, Gerhard-Mercator-University D-47048 Duisburg, Germany and Department of Materials Science, University of North Texas Denton, TX 76203-5308, U. S. A.[Dr.M.H.1]

Received October 10, 1997

Abstract: A overview over some aspects of the statistical theory of rigid and semi-rigid polymers is given starting with Flory's 1956 approach. The main steps of the development of the theory of linear macromolecules are outlined-predominantly, although not consequently, in the historical sequence. Finally, some views on the state of the treatise of non-linear macromolecules are given.

Introduction

High performance polymer[1] based materials have become increasingly important during the last decades as substitutes for conventional - this often means metal based-materials. In certain cases polymer based materials are almost the only choice if certain combinations of properties are required, for example for sandwich printing boards in electronic devices which demand a combination of high electrical resistance, high thermostability, easy processability, minimal expansivity, good adhesion to Cu and high mechanical strength among other qualities. These requirements drew attention on rigid, **rod-like** macromolecules which tend to form oriented anisotropic phases, see for example Fawcett,[2] Ciferri and Ward,[3] Zachariades and Porter[4] or Brostow.[5] They are potential reinforcing additives in conventional plastics, they can form strong high modulus fibres or provide anisotropic, low expansivity materials for special applications. Consequently, in the 70[ies] of this century an intense research started, many new substances and systems have been developed since then, and numerous theoretical papers have been published. However, many facts about these types of substances had been known from early theoretical studies[6-9] which may have appeared first to be of rather academic interest. Now, refinements of

Presented at International Conference on Semi-Rigid Rod Polymeric Materials (October 10-11, 1997, Chosun University, Kwangju, Korea).

these early theories started and further developments of the theories were tackled after these materials had become economical interesting and important.

Some of those new polymer systems can show mesophases, so that there are thermotropic and lyotropic **polymer liquid crystals** (PLCs). Liquid crystallinity is a very important material property affecting the ordering of the polymer chains depending on processing conditions, and hence influencing morphology, anisotropy of the properties, processability, miscibility etc. In PLCs, features of common polymers are combined with the properties of liquid crystals, formerly only known from non-polymeric materials, see Figure 1. Theories[10,11] developed years ago come to new flourishing again and gain attention in areas where this was not expected when the theories were developed.

A big problem was - and still is - that stiff and rigid polymer chains, which provide high mechanical values due to their rod-like character, usually have high melting points though often rather decompose than melt. They tend to be insoluble or only soluble in inconvenient solvents under uncomfortable conditions. This caused different synthetic approaches resulting in **semi-flexible polymers** or otherwise modified rod-like structures, these again gave rise to push theoretical treatments of the systems.

The scientific and technological progress which took place in theory and practice of rigid and semi-rigid polymer systems until today and which is far from being at its end is a good example showing that the studies of prospective scientists (sometimes perhaps "merely" caused by their curiosity to tackle a problem just because it exists, which appear in their time to be only of some academic interest) can rise to enormous economic importance after some time and initiate revolutionary scientific, technological, and economic progress. In the present case this time gap covers about 20 years. More important, it displays the great success of interdisciplinary work and the advantages that arise from looking at more than only a small scientific area and benefiting from the synergistic effects that can be expected.

The aim of this contribution is to give a sketch of the progress in theory and experimental verification in the field of rigid and semi-rigid polymers up to the present state, this is not supposed to be a complete and exhaustive review.

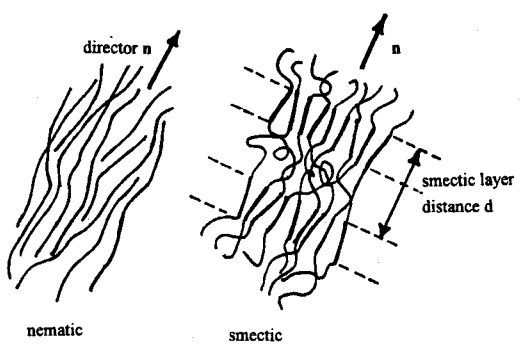

Figure 1. Example of an orientationally ordered state of a polymer. A classification of the different types of PLCs was first given by Brostow,[12] extended by Hess.[13]

First Approach ("1956")

There are different degrees of flexibility or, starting from the other end of the scale, different degrees of rigidity of macromolecules, as schematically shown in Figure 2.

Typical flexible polymers are polysiloxanes, polyethylene or polyphosphazines; a semi-flexible polymer for example is poly(*p*-phenylene terephthalamide), also known by its trade name Kevlar®, the total contour length L is much larger than the Kuhn segment length l, and l is much larger than the diameter d of the chain. A typical rigid-rod-type polymer is poly(*p*-phenylene benzthiazole). Here l is much larger than L, and L is much larger than d. Two mechanisms of flex-

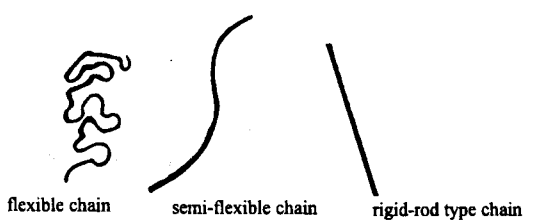

Figure 2. a) flexible polymer chains: bends form over the length of only a few subsequent bonds, b) semi-flexible polymer chains: bends stretch over many bonds, c) rigid rod-like polymer chains: limiting case of vanishing flexibility.

ibility are considered: the freely joined chain and the persistent chain, see Figure 3.

Onsager[8] and Ishihara[9] had predicted spontaneous ordering with phase separation into a highly ordered (') and an isotropic phase ('') for highly asymmetric particles in solution even at low concentrations and in absence of interacting forces. It turned out later that this phenomenon is not restricted to rod-like particles only, the anisotropy of shape can also be of another type, for example discoid.

The lattice method[12,13] is especially attractive for deduction of combinatoric parts of configuration partition functions and had been successfully applied on flexible macromolecules in solution. It had proved to provide reliable semi-quantitative descriptions of polymer solutions.[14,15] After the number of possible conformations that can be placed on the lattice is counted, the configurational partition function Z_M can be calculated for a mixture of macromolecular chains and solvent molecules. Hence, the thermodynamic functions A (Helmholtz free energy), G (Gibbs free energy) or the entropy of mixing can be calculated according to general principles of statistical thermodynamics.[16,17] The lattice consists of cubic cells and each cell can be occupied by either a (quasi-spherical) solvent molecule or a chain segment which is assumed to be equal in size. A segment is further assumed to be of a length equal to its diameter, so that a chain consists of x segments and the length of the extended chain is given by x in segmental units. x is also the number of lattice sites (cells) that are occupied by the polymer chain. It turns out that it is predominantly the length of the polymer molecules that governs the equilibrium properties of solutions of flexible chains. If, however, the polymer chain is comparably stiff or rod-like, randomness in orientation and configurational characteristics of the system at infinite dilution may not prevail at higher concentrations, and states of order as known from monomer liquid crystals (nematic, smectic, chiral phases) may occur at higher concentrations with the corresponding first order transitions. Now, in contrast to flexible polymers, the molecular structure becomes foremost important as long as it influences the flexibility and can surpass the chain length in its influence on thermodynamic properties. The lattice theory is a good tool to deal with the properties mentioned above, even though, it is not the only one.[18-22]

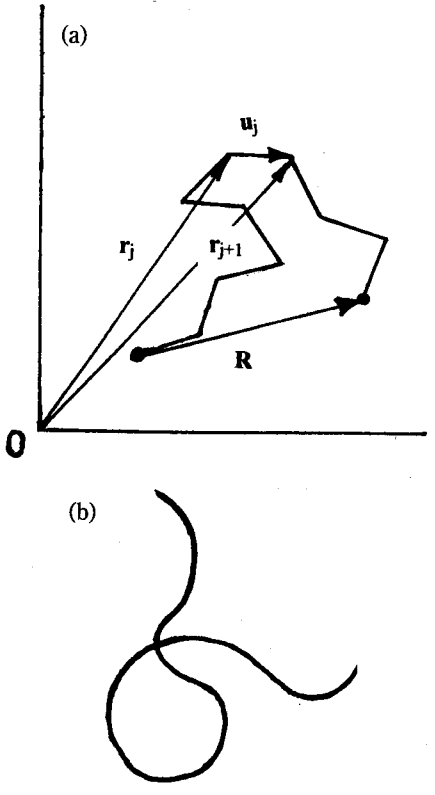

Figure 3. The freely joined chain a) and the persistent chain b).

The intermolecular partition function Z_{inter} (which is also called combinatorial partition function Z_{comb}) is given by:

$$Z_{inter}=\frac{(n_1+xn_2)!\,\zeta^{n_2}}{n_1!n_2!(n_1+n_2)^{(x-1)n_2}} \quad (1)$$

The intramolecular partition function Z_{intra} is given by:

$$Z_{intra} \approx z^{x\cdot n_2} \quad (2)$$

Both combine to the configuration partition function Z_M which is approximated by:

$$Z_M = Z_{inter}\cdot Z_{intra} \approx \left[\frac{(\zeta x)^{n_2}}{e^{(x-1)n_2}\,\upsilon_1^{n_1}\cdot\upsilon_2^{n_2}}\right][z^{x\cdot n_2}] \quad (3)$$

which reduces to $Z_o \approx (\frac{z}{e})^{x \cdot n_2}$ (4)

in the undiluted (bulk) state. n_1 = number of solvent molecules; n_2 = number of solute molecules; ζ = coordination number; x = number of adjacted sites which is equal to the ratio of the molar volumes of solute and solvent if a solute molecule is assumed to be isogeometric with the chain diameter. substitution of x by the number average $<x>_n$ considers the polydispersity of the chain length; z is the partition function attributable to one segment of the long chain. Separabilty of inter-and intramolecular contributions is a direct consequence of the independence of the expected number ν_j of sequences of x adjacent sites on the configuration of flexible molecules. It follows from this separability that the thermodynamics of mixing are independent of the configuration[6,23] and that the spatial configuration does not depend on the composition.[24] Consequently, the configuration of flexible polymer molecules is unaffected by dilution.

Z_{inter} decreases rapidly with increasing concentration and is much smaller than unity at high concentrations, since a lattice site can be occupied only once. On the contrary, Z_{intra} is usually much greater than unity because of the chain flexibility. If the rigidity is too high, Z_{intra} does no longer exceed Z_{inter} so that $Z_M < 1$ and the randomness of the mixture can no longer be accomplished even at low concentrations.

The Gibbs free enthalpy of mixing ΔG_M, respectively the Helmholtz free energy A, is then obtained from eq. 3 after introduction of the Flory-Huggings-Staverman interaction parameter χ by:

$$\Delta G^*_M = RT[n_1 \ln(\upsilon_1) + n_2(\ln \upsilon_2) + \chi x\, n_2 \upsilon_1] \quad (5)$$

n_i are the corresponding moles, υ_i are the volume fractions. The use of the lattice theory usually means constant volume. In addition, it is convenient to have the pressure constant as well, so that the Gibbs function G (synonymous with "Free Enthalpy") is in this case equal to the Helmholtz function A (synonymous with "Free Energy").

The chemical potential of the solvent can then be expressed as:

$$\mu_1 - \mu_{01} = RT\,[\ln(1-\upsilon_2) + (1-\frac{1}{x})\upsilon_2 + \chi \upsilon_2^2] \quad (5a)$$

and correspondingly for the solute:

$$\mu_2 - \mu_{02} = RT\,[\ln(\upsilon_2) - (x-1)(1-\upsilon_2) + \chi(1-\upsilon_2)^2] \quad (5b)$$

Flory started his 1956 approach discussing the behaviour of semi-rigid polymer molecules[6] first, then rod-like particles in solution also using the lattice theory.[7] He introduced a fraction f of isodimensional segments which bend out of the colinear direction which a sequence of completely rigid rods would obtain. He derived:

$$\Delta G_M = \Delta G^*_M + \Delta G_d \quad (6)$$

ΔG_d is the change of the Gibbs free energy observed when perfectly ordered molecules change to the randomly disordered state without directional correlation. With f the equilibrium value of ΔG_d is given by:

$$\Delta G_d = -n_2 RT\left\{\ln x + \ln(\frac{\zeta}{2e}) + (x-2)\ln\left[\frac{1}{(1-2f)e}\right]\right\} \quad (7)$$

A sufficiently small f and high values of x (long chains) yield $\Delta G_M > 0$, indicating the disordered mixture is no longer thermodynamically stable. The bulk polymer ($\upsilon_2 = 1$) will be stable in the disordered state only if the flexibility is so large that the condition $f > 1 - 1/e = 0.63$ is given at sufficiently long chains. The phase transition appears to be a first order transition according to Ehrenfest.[25]

The treatment of rigid rods[7] required the invention of a certain method to place tilted rigid rods on a lattice of cubic cells. Figure 4 shows Flory's procedure.

In a certain sense, however, Flory restricts this lattice approach to large x and small values of ψ_i when he proposes to limit orientations to an average $y/x < 0.5$ since this is "of major interest". In later works, however, these limitations are often neglected, e. g.: when an averaging over ψ_i is done from 0 to $\pi/2$. Since the reasons for these limitations of the molecular orientations are rather mathematical than physical, non-lattice approaches are to be prefered from the physical point of view. The lattice picture, however, at

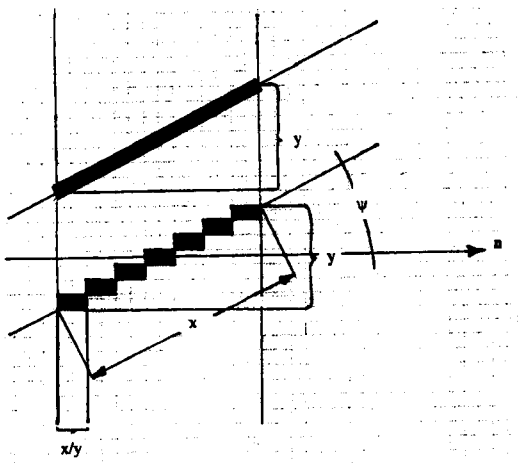

Figure 4. Representation of rods with an angle of inclination (to an axis of preference (director) placed on a cubic lattice (projection in a plane parallel to the director **n**).

least provides a good visual impression and serves quite well within the limits quoted above.

All rods are perfectly ordered when they are parallel with the director **n**. Disorder can then be defined by the projection y_i of the rod's axial ratio x, using the average value y over all orientations. Allowing y to obtain the values 1 (perfect orientation) $\leq y \leq x$ (complete disorder) it is suitable to serve as an index of disorientation,[7] therefore it is called "disorder parameter", sometimes "lattice-model order parameter".

The form of the distribution of the total number of rods, N_x, over the number N_{xy} of molecules attaining disorientations y, given by the ratio N_x/N_{xy} was assumed to be of minor importance in the "1956-approximation"[7] and a simple square-well approximation over the angle range of ψ was chosen. It was taken care of the fact that the average value y was in the limit of complete disorder with $y=x$. The same procedure as outlined above showed that separation into an isotropic and a nematically ordered phase can be expected beyond a critical aspect ratio depending on the concentration. Interparticle forces except repulsion on contact were excluded in this treatment. For the anisotropic, ordered phase (')

$$(\mu_1-\mu_{01})'=RT\left[\ln(1-v'_2)+\left(\frac{y-1}{x}\right)v'_2+\frac{2}{y}+\chi v'^2_2\right] \tag{8}$$

is obtained, while the corresponding expression for the isotropic phase ('') is identically with eq. 5a for long chains, since $y=x$ is valid in the disordered phase. The corresponding results for the solute are:

$$(\mu_2-\mu_{02})'=RT\left[\ln\left(\frac{v'_2}{x}\right)-(y-1)v'_2+2-\ln y^2+\chi(1-v'_2)^2\right] \tag{9a}$$

$$(\mu_2-\mu_{02})''=RT\left[\ln\left(\frac{v''_2}{x}\right)-(y-1)v''_2+2-\ln y^2+\chi(1-v''_2)^2\right] \tag{9b}$$

The equilibrium conditions are obtained from the condition:

$$\mu'_j=\mu''_j \tag{10}$$

so that phase diagrams can be calculated, $\chi=0$ means the **athermal** case, see for example Figures 5, 6, and 7.

Application of the equilibrium condition (eq. 10) on the example in Figure 5 gives mathematical solutions for $0.055<\chi<0.08$. A minimum and a following maximum indicate a possible existence of a two-phase equilibrium - the isotropic phase '' and the dilute anisotropic phase '.

Plotting the interaction parameter χ versus the composition (at constant temperature), the phase diagram - Figure 6 - is obtained which can be converted into the familiar composition vs. tem-

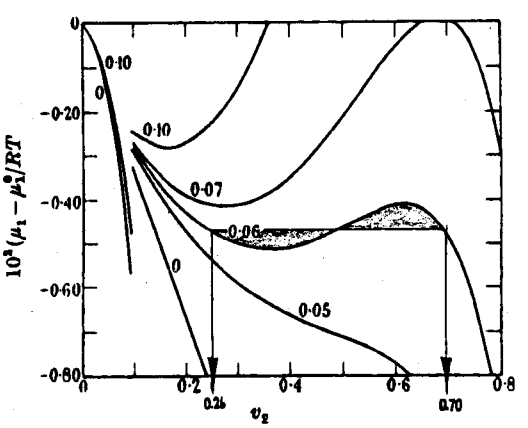

Figure 5. Chemical potential as a function of the concentration at a fixed chain length $x=100$ and exotherm enthalpies of mixing indicated by the corresponding values of the Flory-Huggins-Staverman-polymer-solvent interaction parameter χ. After ref. 7. Reproduced with permission of the Royal Society, London.

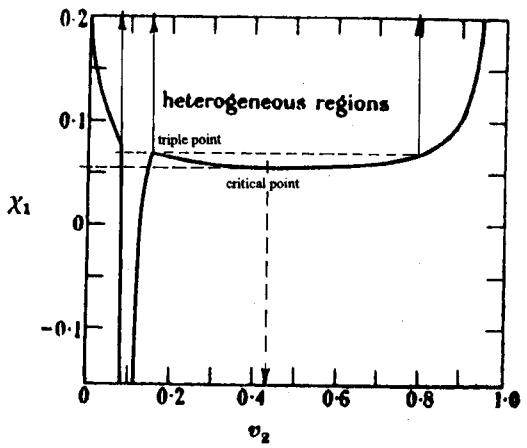

Figure 6. Composition of phases at a fixed chain length $x = 100$ vs. the interaction parameter χ. After ref. 7 with permission of the Royal Society, London.

perature diagram if $\chi(T)$ is known.

Although it is only a crude approximation - see below - the predictions of this theory have been found in some qualitative agreement with experimental findings, for example by Hermans,[26] Wee and Miller[27] (helical peptides), or Morgan e. a.[28] and Papkov e. a.[29] (synthetic polymers). However, detailed studies by Straley[30] showed that it leads to inconsistencies and does not predict phase separation of an anisotropic phase even at very high aspect ratios. Flory and Ronca[31] showed that this deficiency is due to an incorrect relation of y and the angular disorientation of the rod-like particles.

Further Refinements

The exact treatment of the disorientation parameter y and the spatial distribution of the rods by Flory and Ronca[33] resulted in more sophisticated equations for the average value:

$$\bar{y} = n_x^{-1} \sum_y y\, n_{xy} \tag{11}$$

which is calculated from:

$$\bar{y} = \frac{4}{\pi} x \frac{f_2}{f_1} \tag{12}$$

with f_1 and f_2:

$$f_1 = \int_0^{\frac{\pi}{2}} \sin \Psi \exp[-(\alpha \sin \Psi)]\, d\Psi,$$

$$f_2 = \int_0^{\frac{\pi}{2}} \sin^2 \Psi \exp[-(\alpha \sin \Psi)]\, d\Psi \tag{13a,b}$$

$$\alpha = \frac{4}{\pi} a x \tag{13c}$$

and

$$a = -\ln[1 - v_x(1 - \frac{\bar{y}}{x})] \tag{13d}$$

so that the average over all the sin Ψ is given by:

$$< \sin \Psi > = \frac{f_2}{f_1} \tag{14}$$

$$\text{hence: } \bar{y} = \frac{4}{\pi} x \frac{f_2}{f_1} = \frac{4}{\pi} x < \sin \Psi > \tag{15}$$

for random orientation of the rods with $f_1 = 1$ and $f_2 = \pi/4$.

Eq. 12 and 13 indicate homogeneous solutions only for volume fractions v_x greater than the limiting value, which depends on x. At concentrations beyond this limiting value the phase separa-

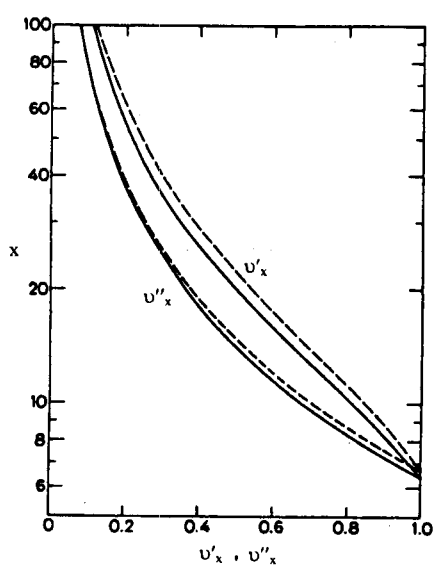

Figure 7. Equilibrium volume fractions v_x' (ordered phase) and v_x'' (isotropic phase) of athermal solutions as a function of the axis ratio x[33]. The solid lines describes the coexistence calculated according to the exact treatment, the dashed curves correspond to the "1956-approximation".[7] Reprinted with permission of Gordon & Breach Sci. Publ.

tion is observed. Figure 7 shows the situation in an athermal system in comparison with the 1956 approach.

Further Development of the Theory: the 1978 Series

Already in 1978[32-37] a series of papers were published by Flory an co-workers who further refined the theory, namely - in the order quoted above: the theory of polydisperse rod-like systems, the theory of ternary systems (two rod-like polymers with different aspect ratios and a solvent), mixtures of solvent and rods where the rods obey a "most probable distribution", where they obey a Poisson distribution, ternary mixtures of solvent, rigid rods and (flexible) random coil polymers, and finally, rods connected by flexible joints. Non-combinatorial contributions to the partition function were omitted throughout this series of papers.

The theory of polydisperse systems[34] in which Flory and Abe treated systems consisting of a quasi spherical solvent and rod-like particles with polydisperse aspect ratios. They did calculation of the corresponding phase equilibria, and studied[35] the influence of the degree of polymerization of a (rod-like) polymer A in a solution containing the rods B.

The general procedure is as outlined above except that there is a distribution y_x of y caused by the diverse x-mers. The partition function is given by:

$$-\ln Z_M = n_1 \ln \upsilon_1 + \sum n_x \ln \upsilon_x - (n_1 + \sum x n_x)\left[1 - \upsilon_2\left(1 - \frac{\bar{y}_n}{\bar{x}_n}\right)\right] \ln\left[\left(1 - \frac{\bar{y}_n}{\bar{x}_n}\right)\right] - \sum n_x [\ln(x y_x^2) - (y_x - 1)] \quad (16)$$

With $\upsilon_2 = \sum \upsilon_x$ (16a), $\bar{x}_n = \frac{\sum x n_x}{\sum n_x}$ (16b), $\bar{y}_n = \frac{\sum y_x n_x}{\sum n_x}$ (16c). Eq. 16b, c define the number averages of x and y, respectively.

Now, the cases $\mathbf{y} \leq \mathbf{x}$ and $\mathbf{y} > \mathbf{x}$ have to be distinguished. The first condition is valid for aligned species whose orientations are positively correlated with the director - they will be indexed "A". The second condition comprises random species, which are not oriented having a random distribution-they will be indexed "R".

The chemical potential of the solvent is then given by:

$$(\mu_1 - \mu_{01}) = RT\left[\ln(1-\upsilon_2) + \frac{2}{y} + \upsilon_{2R}\left(1 - \frac{1}{\bar{x}_{nR}}\right) + \upsilon_{2A}\left(\frac{y-1}{\bar{x}_{nA}}\right)\right] \quad (17)$$

The chemical potential of the polymer is given by:

$\mathbf{x} \leq \mathbf{y}$:

$$(\mu_x - \mu_{0x}) = RT\left[\ln\left(\frac{\upsilon_x}{x}\right) + \frac{2x}{y} - \ln x^2 + x\upsilon_{2R}\left(1 - \frac{1}{\bar{x}_{nR}}\right) + x\upsilon_{2A}\left(\frac{y-1}{\bar{x}_{nA}}\right)\right] \quad (18)$$

$\mathbf{x} > \mathbf{y}$:

$$(\mu_x - \mu_{0x}) = RT\left[\ln\left(\frac{\upsilon_x}{x}\right) + 2 - \ln x^2 + x\upsilon_{2R}\left(1 - \frac{1}{\bar{x}_{nR}}\right) + x\upsilon_{2A}\left(\frac{y-1}{\bar{x}_{nA}}\right)\right] \quad (19)$$

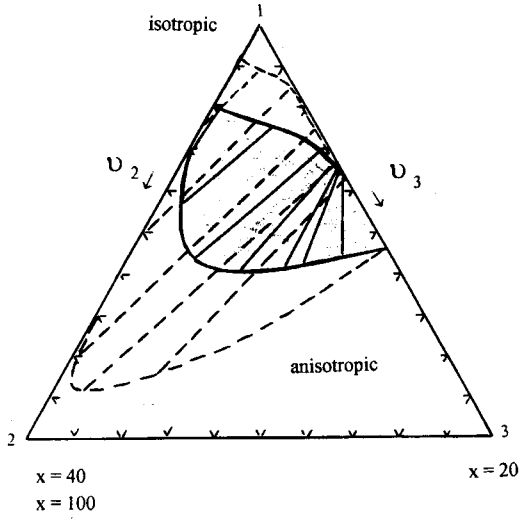

Figure 8. Calculated ternary phase diagram of a system comprising the solvent 1-aspect ratio $x_1 = 1$ and the two dissolved species: rod-like polymer 2 - $x_2 = 40$ (solid curves) or $x_2 = 100$ (broken curves), rod-like polymer 3 - $x_3 = 20$. The solution is athermic ($\chi = 0$). The miscibility gap is given by the binodals, some representative tie lines indicate the composition of coexisting phases. The coordinates putting up the Gibbs triangle are the volume fractions υ of the components. The biphasic region increases with increasing difference of the polymer aspect ratios. There is also evidence for a triphasic coexistence of one isotropic phase with two anisotropic phases.[35] Figure redrawn from values given in.[35] Reproduced with permission of The American Chemical Society.

For an isotropic phase results:

$$(\mu_1-\mu_{01})''=RT\,[\ln(1-\upsilon''_2)+\upsilon''_2(1-\frac{1}{\bar{x}_n})] \quad (20)$$

$$(\mu_x-\mu_{0x})''=RT\,[\ln(\frac{\upsilon''_x}{x})+x\upsilon''_2(1-\frac{1}{\bar{x}_n})-\ln x^2] \quad (21)$$

Numerical calculations of ternary phase diagrams are shown in Figure 8.

Consequently, the next step was the study of ternary mixtures comprising solvent, rod-like-and random-coil polymers[38] by adapting the procedure developed in.[34] The resulting partition function is:

$$-\ln Z_M=n_1\ln\upsilon_1+n_2\ln\upsilon_2+n_3\ln\upsilon_3$$
$$n_0\left[1-\upsilon_2(1-\frac{y}{x_2})\right]\ln\left[(1-\frac{y}{x_2})\right]+(n_2y-1)$$
$$-n_2\ln(x_2y^2)+n_3(x_3-1)-n_3\ln(x_3y_3) \quad (22)$$

with the definition: $n_0=n_1+x_2n_2+x_2n_2$ (22a) and z_3 the internal partition function of the random coil polymer. The indices 1, 2, and 3 correspond to the solvent, the rod and the coil, respectively. The chemical potentials for an anisotropic phase (') (athermal) are given by:

$$(\mu_1-\mu_{01})'=RT\,[\ln\upsilon'_1+\frac{\upsilon'_2(y-1)}{x_2}\upsilon'_3(1-\frac{1}{x_3})+\frac{2}{y}] \quad (23a)$$

$$(\mu_2-\mu_{02})'=RT\,[\ln(\frac{\upsilon'_2}{x_2})+\upsilon'_2(y-1)+\upsilon'_3x_2(1-\frac{1}{x_3})+2(1-\ln y)] \quad (23b)$$

$$(\mu_3-\mu_{03})'=RT\,[\ln(\frac{\upsilon'_3}{x_3})+\upsilon'_2\frac{x_3}{x_2}(y-1)+\upsilon'_3(x_3-x_1)+\frac{2x_3}{y}-\ln z_3] \quad (23c)$$

and for the isotropic phase (''):

$$(\mu_2-\mu_{02})''=RT\,[\ln\upsilon''_1+\upsilon''_2(1-\frac{1}{x_2})+\upsilon''_3(1-\frac{1}{x_3})] \quad (24a)$$

$$(\mu_2-\mu_{02})''=RT\,[\ln(\frac{\upsilon''_2}{x_2})+\upsilon''_2(y-1)+\upsilon''_3x_2(1-\frac{1}{x_3})-\ln x_2^2] \quad (24b)$$

$$(\mu_3-\mu_{03})''=RT\,[\ln(\frac{\upsilon''_3}{x_3})+\upsilon''_2x_3(1-\frac{1}{x_2})+(\upsilon_3x_3-1)-\ln z_3] \quad (24c)$$

The equations 23 and 24 can be used to calculate the phase diagram.[38] Figure 9 shows isothermal phase diagrams of ternary athermal systems and the influence of the degree of polymerization x.

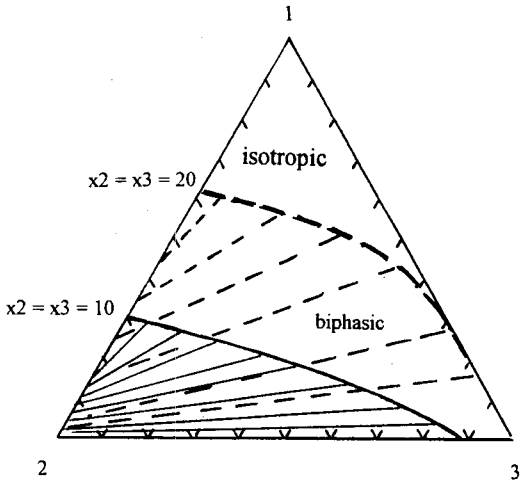

Figure 9. Ternary phase diagrams comprising solvent - component 1, rigid rod polymer - component 2 - with $x_2=10$, and component 3 - the random coil polymer - $x_3=10$ (solid lines), and $x_2=x_3=20$ (broken lines). Along the thick lines (binodal) there is a two-phase equilibrium of the coexisting isotropic and anisotropic phase, some tie lines are shown exemplary as thin lines. Redrawn with values from ref 38 with permission of The American Chemical Society.

The random coil polymer (3) is in the whole concentration range miscible with the solvent (1) and partially miscible with the rod (2). Below $\upsilon_3\cong 0.88$ there is no miscibility and the miscibility gap becomes larger with increasing x. The solution of the rod-like polymer decomposes into an isotropic and an anisotropic (ordered) phase beyond $\upsilon_2\cong 0.7$. Increasing chain length increasingly expels the rods from the isotropic solution. This is caused by the primary differences of their partition functions and the isotropic solution offers none of the advantages of the oriented phase. Consequently, the rods prefer the oriented phase already at quite low concentrations because the ordered phase mitigates obstruction by neighbouring species by mutual alignment comparable with logs on a lake, rejecting the coils. The most prominent properties of these diagrams may be summarized as follows:

- the addition of a coil polymer to the binary mixture solvent + polymer rods increases the polymer volume fraction of the anisotropic

phase.

- there is a biphasic area which decomposes into an anisotropic phase that contains solvent and rod polymer but practically no coil polymer, and an isotropic phase that contains the whole coil polymer, solvent and rod polymer. A higher overall polymer concentration means a higher degree of polymer segregation.

The prediction of the theory has been confirmed by results published by Aharoni[38,39] and Hwang.[40] Bianchi and co-workers[41] investigated the system: solvent dimethylacetamide + LiCl, rigid rod polymer poly(*p*-benzamide) (PBA), and coil polymer poly (terephthal-*p*-aminobenzhydrazide) (PAHB-T), which could be described qualitatively by Flory's expressions.[38] In particular, the exclusion of the coil polymer from the ordered phase was verified. Systems containing incompatible (endothermal) polymer combinations, however, show completely different phase diagrams because of phase separation already in the isotropic state without formation of an ordered phase.[42,43] Also triphasic equilibria were observed.

Real polymers exhibit always a certain degree of flexibility because of the cumulative deviation from strict rectilinearly through a certain bending of bond angles and they have to be characterized by a finite persistence length. Hence, rod-like molecules can be represented in a simple approximate model by straight segments interconnected with each other by joints that exhibit a certain degree of flexibility because they allow certain deviations of the bond angle, thus introducing some degree of randomness into the otherwise stiff chain.[39] A logical continuation the is to substitute the flexible joints by flexible chains.[44,45] A further development of the theory was, to extend it to chains with interconvertible rod-like and random-coil sequences to describe helix-coil transitions.[46] The method applied was again the same as already referred to.[7,34,38] It turned out that polymer chains formed by connecting rigid rods with flexible connections show isotrop-anisotrop phase equilibria almost coinciding with those of a system of disconnected rods of the same dimensions. Connecting the rods with (fixed) localized flexible sections of random coils, however, should show significant effects.

The partition function of m flexibly joined rods was obtained as:

$$-\ln Z_M = n_1 \ln v_1 + n_1 \ln\left(\frac{v_2}{x_m}\right) - (n_1 + x_m n_2)\left[1 - v_2\left(1 - \frac{y}{x}\right)\right] \ln\left[1 - v_2\left(1 - \frac{y}{x}\right)\right] - n_2(m \ln y^2 - my + 1) \quad (25)$$

Compared with eq. 16 - the partition function of polydisperse rods - the main difference occurs in the last term. The chemical potentials are then given by:

$$(\mu_1 - \mu_{01}) = RT\left[\ln(1 - v_2) + \frac{2}{y} + v_2\left(\frac{y}{x} - \frac{1}{x_m}\right)\right] \quad (26)$$

$$(\mu_2 - \mu_{02}) = RT\left[\ln\left(\frac{v_2}{x_m}\right) + v_2 x_m\left(\frac{y}{x} - \frac{1}{x_m}\right) + 2m(1 - \ln y)\right] \quad (27)$$

from which the chemical potentials for the isotropic solution ('') ($y = x$, with $x >> 1$) is obtained:

$$(\mu_1 - \mu_{01})'' = RT\left[\ln(1 - v''_2) + v''_2\left(\frac{y}{x} - \frac{1}{x_m}\right)\right] \quad (28)$$

$$(\mu_2 - \mu_{02})'' = RT\left[\ln\left(\frac{v''_2}{x_m}\right) + v''_2(x_m - 1) - 2m \ln x\right] \quad (29)$$

A comparison with eq. 20 and 21 shows the difference to the unconnected rods. The overall chain length $x_m = mx$ has only a minor influence on the phase separation, since the concentration regime depends on the chain length and the separation of an ordered phase into an isotropic and an anisotropic phase requires to be well above that regime. However, the chain length dependence of μ is at incident concentrations superseeded by interactions of higher order and hence becomes of secondary importance. The length of a rigid segment is of greater influence than the overall chain length.

The partition function of a chain composed of rod-like segments and random coil segments in the backbone of the macromolecule is derived from a suitable representation of the semi-rigid chain on the lattice, see Figure 10. In terms of Brostow's classification[12,13] this is a longitudinal polymer liquid crystal (PLC), provided it shows mesophases.

The flexibility of this type of macromolecule is caused by the presence of occasional structural

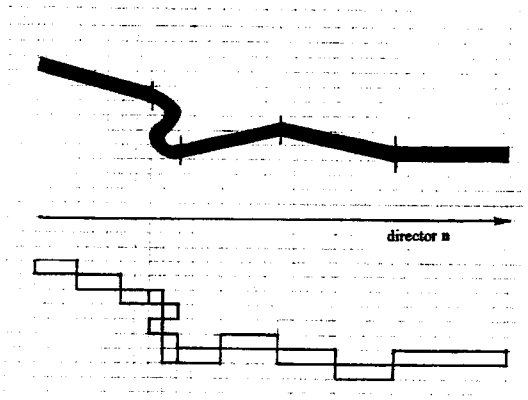

Figure 10. Representation of a semirigid chain comprising four rod-like subchains and one flexible subchain, each of them consisting of sequences which are formed by segments. One segment occupies the same volume as a solvent molecule, i. e. one lattice site. The first subchain from the left is rigid and consists of 3 sequences, so that $y_i^{(1)} = 3$. The second subchain from the left is flexible, all the other subchains are rigid and can be liquid crystalline. The higher the local value $y_i^{(i)}$ the larger is the deviation of the given subchain from the director **n**. For the fifth subchain from the left therefore $y_j^{(5)} = 1$ is valid since it is parallel to the director and the abscissa of the lattice.

or conformational irregularities that force abrupt deviations from the director. Flexibility may also be caused from cumulative effects of small deviations. Matheson and Flory's treatment[46] dealt with the former case.

The partition function of a mixture of a polymer consisting of macromolecules as sketched in Figure 10 contains - besides the familiar combinatoric (steric) factor and the orientational contribution-a third exponential factor which introduces the free energy of interaction between solvent and solute:

$$Z_M = Z_{comb} Z_{orient} \exp(-\chi v_1 \sum_x x n_x) \qquad (30)$$

Application of the familiar procedure yields for the isotropic mixture:

$$(\mu_1 - \mu_{01})'' = RT\,[\ln(1-v'_p) + (1-\frac{1}{x})x\,v''_p + \chi v''^2_p] \qquad (31)$$

and

$$(\mu_x - \mu_{0x})'' = RT\,[\ln(\frac{v''_x}{x}) + (1-\frac{1}{x})x\,v''_p - (x - \sum_\eta \eta\gamma_{x\eta})\ln z_c - \sum_\eta \gamma_{x\eta} \ln \eta^2 + x\chi(1-v''_p)^2] \qquad (32)$$

v_p'' is the volume fraction of the polymer, $\bar{x}$ is the number average of the chain length, $\gamma_x\eta$ is the number of rigid sequences which have the segment length η in a molecule of the size x, and z_c is the internal configuration partition function of the coil. It is worth mentioning here that the allocation of the flexible subchains appears to be of no importance, it is their total number that determines the thermodynamics.

Figure 11 clearly shows the influence of the flexible subchains: they decrease the width of the biphasic gap markedly as long as $\chi > 0$ is valid. This influence is only small if $\chi < 0$. The presence of flexible subchains increases the disorder parameter y at a given χ-parameter in the anisotropic phase with a pronounced effect at long-

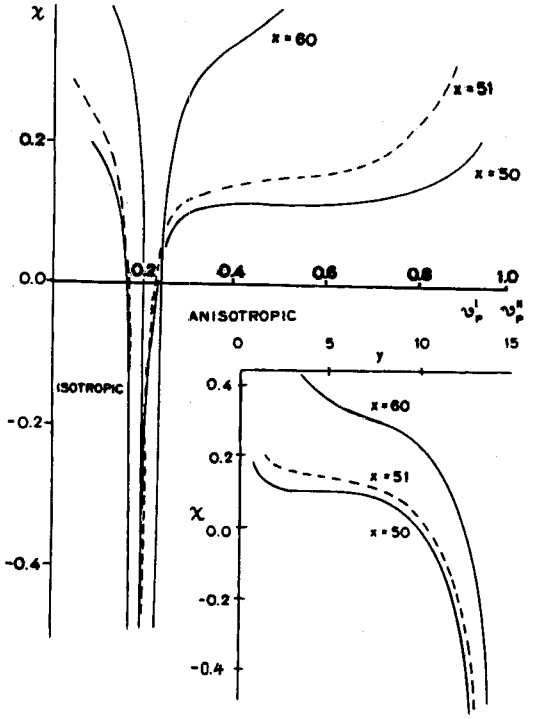

Figure 11. Phase diagram of a binary system solvent/semiflexible polymer. The polymer consists of a rigid subchain with aspect ratio 50 and appended tails of 0, 1 or 10 randomly coiled subchains, as indicated. The polymer is assumed to be monodisperse. The small figure shows the relation between the disorder parameter y and the Flory-Huggins-Staverman polymer-solvent interaction parameter $\chi(T)$. After Matheson & Flory[46] with permission of The American Chemical Society.

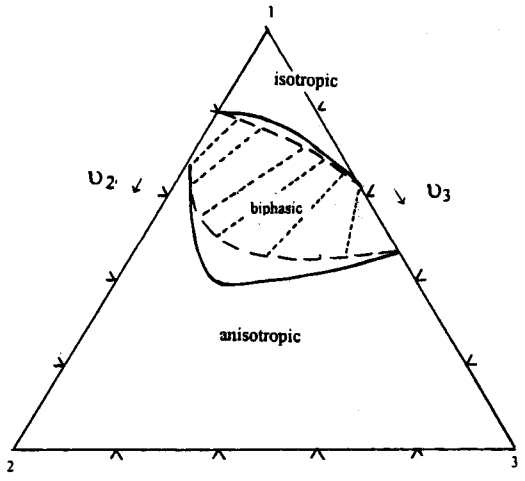

Figure 12. Influence of the modification of the rod-type molecules in a ternary, athermal system comprising rods, coiled polymers and solvent. The solid curves are the binodals of the (simple) rod containing system with $x_a = \eta_a = 40$ and $x_b = \eta_b = 20$, the broken lines are the binodals of the modifies rods containing system with one flexible subchain and otherwise unaltered properties, hence $x_a = \eta_a = 39$ and $x_b = \eta_b = 20$. Redrawn after ref. 46 with permission of The American Chemical Society.

er flexible subchains.

Figure 12 shows the influence of introducing flexible subchains attached to rods present in ternary systems comprising rods, coiled macromolecules and solvent.

The significant decrease of the biphasic gap caused by the presence of only one flexible subchain on the rigid rods. Again, depending on the composition of the components and the mixture triphasic equilibria can be observed. Fractionation of the rods via accumulation in the anisotropic phase are suppressed by the presence of a sufficient amount of flexible subchains. Restrictions of the theory are given by the condition that about 10-20 flexible bonds have to be present to provide sufficient independence of the motions and that the rod like subchains have to be sufficiently long.

Considering Orientation-dependend Interactions

The theoretical approaches presented up to this point have dealt with systems without any interchain interaction, except that they cannot interpenetrate. It is, however, well known from the theory of liquid crystals that consideration of anisotropic pair-pair interactions provides description of thermotropic mesophase behaviour.[10,11] The orientation dependent-hence anisotropic-interaction is the result of the anisotropy of the dispersive interactions of the molecules. Focusing only on anisotropic attractive forces due to molecules with anisotropic polarizabilities, Maier and Saupe[10,11] could describe properties of nematic phases neglecting steric or space filling effects of nematogens. Flory and Ronca[47] extended their treatment of rigid rod systems by combining orientation-depending interaction energies between neighbouring pairs of subchains with the partition function for non-interpenetrable rigid rods derived earlier. The fraction of particles with the equilibrium orientation described by y is given by:[33]

$$\frac{n_{xy}}{n_x} = \frac{1}{f_1}\omega_y \exp(-ay) \tag{33}$$

with the factor a defined by eq. 13d and ω_y meaning a priory probability for the interval of orientations associated with the disorder parameter y. Taking into account now anisotropic energetic interactions of the Maier-Saupe type, the left hand fraction of eq. 33 becomes:[11]

$$\frac{n_{xy}}{n_x} \propto \omega_y \exp[-\alpha \sin\Psi_y + s\tilde{T}^{-1}(1-\frac{3}{2}\sin^2\Psi_y)] \tag{34}$$

where s is Hermans order parameter[48,49]

$$s = 1 - \frac{2}{3} < \sin^2\Psi > \tag{35}$$

and the reduced temperature $\tilde{T} \equiv \frac{T}{T^* \cdot x}$ (36)

where T^* has the meaning of a characteristic temperature given by:

$$T^* \propto r^{*-6}(\Delta\beta)^2 \tag{37}$$

$\Delta\beta$ describing the difference between the polarizabilities along and normal to the cylindrical axis of a rigid particle or subchain and r^* the distance between the interacting particles. α is given by:

$$\alpha = -(\frac{4}{\pi})\ln(\frac{\bar{y}}{x}) \tag{38}$$

which is obtained from eq. 13c, d with $\upsilon_x = 1$.

The normalization factor $\frac{1}{f_1}$ for eq. 34 can now be defined in a more general way:

$$f_j = \int_0^{\frac{\pi}{2}} \sin^j \Psi \exp[-\alpha \sin\Psi - \frac{3}{2} s\widetilde{T}^{-1} \sin^2\Psi] d\Psi \quad (39)$$

$$j = 1, 2, 3$$

see also eqs.13a, b but incorporating the term esp $[s\widetilde{T}^{-1}]$ now. The eqs.12 and 14 are obtained again and in addition:

$$\frac{f_3}{f_1} = <\sin^2\Psi> = \frac{2}{3}(1-s) \quad (40)$$

The Helmholtz free energy for a neat liquid ($\upsilon_1 = 0$, $\upsilon_x = 1$) is then given by:

$$A = n_x kT\left[\underbrace{\bar{y} - 1 - s\left(1 - \frac{s}{2}\right)\widetilde{T}^{-1}}_{a} - \underbrace{\ln x\, \sigma f_1}_{b}\right] \quad (41)$$

a result which differs from Maier-Saupe[11] in the terms a and b. In the isotropic case ($s = 0$, $f_1 = 1$, $\bar{y} = x$) eq. 41 reduces to:

$$A_{iso} = n_x kT[x - 1 - \ln x\, \sigma] \quad (42)$$

where σ denotes an arbitrary parameter which is often chosen in a way so that the statistical weight for the perfect order with the condition $y = 1$ is also unity.[7,34,48]

The biphasic equilibrium of isotropic and anisotropic phases can be derived now from the identity of eqs. 41 and 42. Discussion of the equilibrium conditions shows that there is an almost identical $s \approx 0.44$ for **monomeric** nematics at the isotropic/anisotropic equilibrium temperature. Numerical calculations basing on the equations derived by Flory and Ronca show an increase of the order parameter with growing aspect ratio at the transition temperature, starting at $x = 0$ at the Maier-Saupe limit, approaching $s = 1$ for $x > 6$. The theory clearly presents the great influence of the aspect ratio. Numerous experimental results[49] on nematics that are approximately rigid rod like of structure display that there are good reasons that characteristics of the nematic-isotropic transition can be quantitatively correlated with molecular structure. The molecular orientation can result in an order parameter $0 > s > -1/2$ if the director **n** is predominantly orthogonal with respect to the optical axis of the sample. This is a special case of a cho-

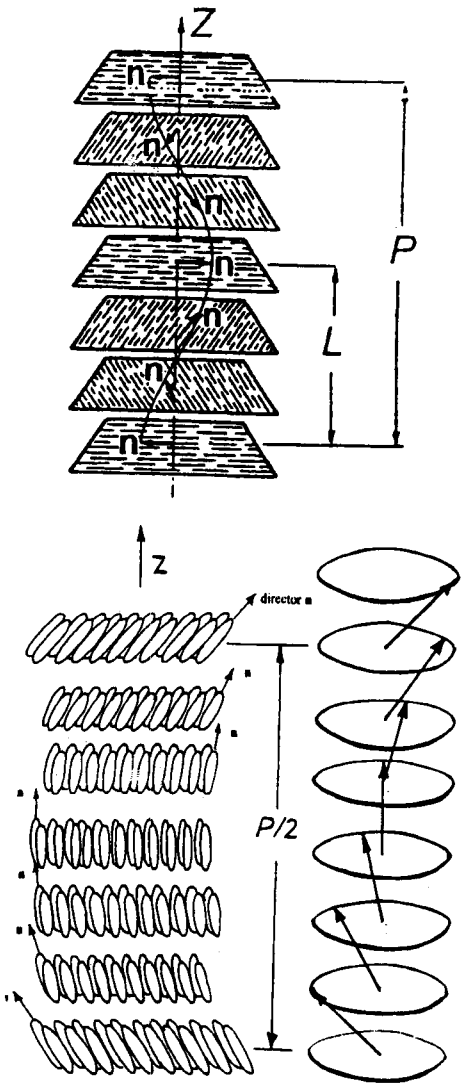

Figure 13. Cholesteric phases a) chiral nematic N* In a N* phase, the director **n** precesses about an axis z, e. g: the axis of optical anisotropy. This mesophase is locally similar to an uniaxial nematic except for the precessing of the director. The structure is periodic along z and the spacial period L is equal to 1/2 of the pitch P of the helical structure. b) chiral smectic C*. S_c* is a phase with a helical structure in which each successive layer is rotated through a certain angle relative to the preceding one so that a twisted structure with the pitch P is formed. Locally, the structure is essentially the same as that of the achiral S_c except that there is a precession of the tilt direction about the z axis. Definition according to a IUPAC document in preparation on the nomenclature of liquid crystals.

lesteric mesophase, namely chiral nematic, see Figure 13. The Helmholtz free energy of such a system is always higher than in a system with nematic structure. It will be shown later[50] that this metastable phase can be stabilized by the presence of flexible subchains in a semi-rigid polymer without having to assume biaxiality of the orientational interactions. Chiral nematic phases were described with such additional conditions by earlier theories, for example by Varichon and Ten Bosch.[51,52]

Recent Developments

In the absence of internal interactions the Matheson-Flory theory can be used,[46] Flory and Ronca[49] take into account orientational interactions. In 1993 a study was published by Brostow and co-workers who combined both and treated the influence of concentration and length of the rigid subchains in semi-rigid polymer systems with anisotropic interactions. In the first part they focus on the bulk properties,[53] on the properties of mixtures in the following part,[54] and special attention is drawn on the isotropic-anisotropic transition in the third part.[55]

Each polymer molecule consists of r segments. r_c of them form coiled subchains and r_h form rigid subchains. The combination of alternating rigid and flexible subchains form the macromolecule with a degree of polymerization r, so that the following equations are valid:

$$r = r_c + r_h = n(\eta_c + \eta_h) \tag{43}$$

$\bar{\eta}$, which is used later is the average length of a subchain as indexed in each chain, it is equivalent to the axis ratio x. For simplicity, the unindexed symbol is later used for rigid subchains. Then the fraction θ can be defined:

$$\theta = \frac{r_h}{r} \tag{44}$$

which serves as a measure of the composition. Provided there are no vacant sites on the cubic lattice, the number N of lattice sites is given by the number of polymer molecules N_p and the degree of polymerization:

$$N = N_p r \tag{45}$$

The model is similar to parts of Figure 10. The partition function Z again is the product of the combinatoric and the orientational part as in eq. 30 without the solvent interaction part, however.

The Helmholtz function $\tilde{A}$ per molecule is then given by:[18,19]

$$\tilde{A} = -kT(\ln Z_{comb} + \ln Z_{orient}) \tag{46}$$

Following the familiar Flory procedure and using the Flory-Irvine[56] expression for Z_{orient} there is:

$$\frac{\tilde{A}}{N_p kT} = -\frac{1}{N_p}(\ln Z_{comb} + \ln Z_{orient}) =$$

$$\underbrace{\ln\frac{1}{r} + r\left\{(1+\frac{1}{r}) - (1-Q)\ln(1-Q) - Q - 1 - Q\ln q_c\right\}}_{\text{combinatoric term}} -$$

$$\underbrace{\frac{n\bar{\eta}}{N_p}\left\{\ln f_1 + \gamma\langle\sin\Psi\rangle + \theta s\,\tilde{T}^{-1}(1-\frac{s}{2})\right\}}_{\text{orientational term}} \tag{47}$$

$$\text{with: } Q = \theta(1-\frac{\bar{y}}{\bar{\eta}}) = \theta(1-\frac{4f_2}{\pi f_1}) \tag{48}$$

$$\text{and: } \bar{y} = \frac{1}{(j-1)\frac{\theta r}{\bar{\eta}}}\sum_{i}^{j-1} y_i \tag{49}$$

Coexistence of the anisotropic and the isotropic phase requires

$$\tilde{A}_{aniso} = \tilde{A}_{iso} \tag{50}$$

with the conditions for the isotropic phase: $s = 0$ and $\bar{y} = \bar{\eta} \rightarrow Q = 0$ and $f_1 = 1$, so that the basic equation:

$$\bar{\eta}(1-\theta)\ln(1-Q) + \bar{\eta}Q + \theta\left\{\ln f_1 + \theta s\,\tilde{T}^{-1}(1-\frac{s}{2})\right\} = 0 \tag{51}$$

is obtained. Q is defined by eq. 48, s by eq. 40 and the f_j are given by a slightly modified eq 39 now:

$$f_j = \int_0^{\frac{\pi}{2}} \sin^j\Psi \exp[-\gamma\sin\Psi - \frac{3}{2}\theta s\,\tilde{T}^{-1}\sin^2\Psi]d\Psi \tag{52}$$

$$j = 1, 2, 3$$

$$\gamma = -\frac{4}{\pi}\ln(1-Q) \tag{53}$$

where α - eq. 38 - has changed to γ - eq. 53 - now, and the composition θ has been introduced. Eq.

53 becomes identical with eq. 38 derived by Flory and Ronca if the copolymer reduces to a system of pure rigid rods of the length $x = \bar{\eta}$ where $\theta = 1$ is valid. The ratio $\frac{\theta}{\tilde{T}}$ has already been introduced by Flory and Ronca[49] and measures the intensity of orienting interactions between hard subchains and the orienting molecular field, as can be concluded from the Maier-Saupe theory:

The sum of interactions between dipoles in a system is replaced by interactions between the dipole under consideration and a molecular mean field. If the dipoles are of cylindrical geometry the interaction energy ε between a dipole and the mean field is obtained after averaging over all orientations of the dipole under consideration taking into account only the nearest neighbours-interactions. The interaction energy ε is proportional to a term $\zeta C \cdot r^{*-6}$. ζ is the number of nearest neighbours, C is a positive potential constant measuring the intensity of interactions between a pair of dipoles and has negligible temperature dependence. C is assumed to be proportional to θ and $\bar{\eta}$, so that $\frac{\theta}{\tilde{T}}$ becomes proportional to ε.

Practical use of the equations derived above requires the solution of a set of equations G_j:

$$G_j(\gamma, s, \bar{\eta}, \tilde{T}^{-1}, \theta) \qquad (54)$$
$$j = 1, 2, 3$$

with:

$$G_1 \equiv \bar{\eta}(1-\theta)\ln(1-\theta)\bar{\eta}Q + \theta\left\{\ln f_1 + \theta s \tilde{T}\,(1-\frac{s}{2})\right\} \qquad (54a)$$

$$G_2 \equiv \gamma + \frac{4\bar{\eta}}{\pi}[\ln(1-Q)] \qquad (54b)$$

$$G_2 \equiv \frac{2}{3}(1-s) - \frac{f_3}{f_1} \qquad (54c)$$

The equations 54 can be solved after having chosen a realistic value for one of the four variables. $\bar{\eta}$, for example can be determined by small angle neutron scattering.[57]

Flory and Matheson[46] had shown that with increasing axial ratio η of rod-type subchains in the macromolecules a higher amount of random oriented subchains is tolerated, see Figure 14.

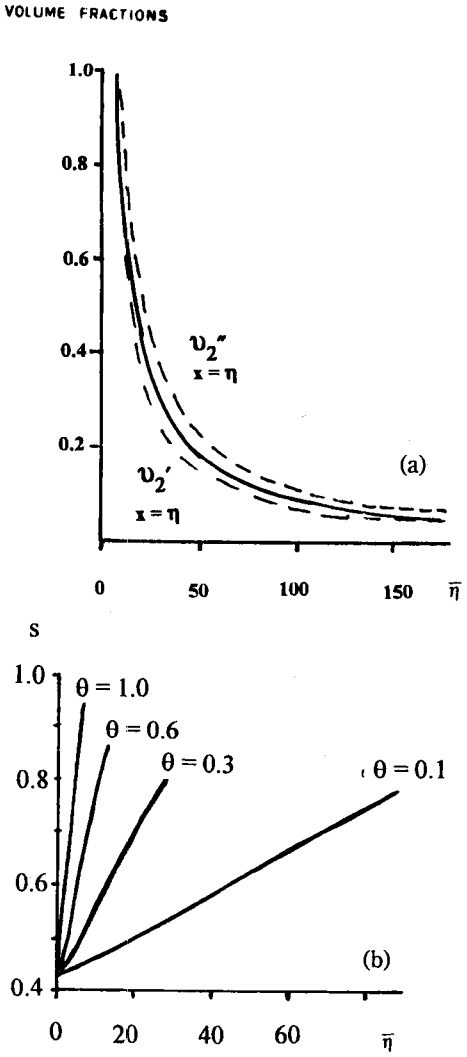

Figure 14. a) volume fractions υ_p of the polymer in the anisotropic phase ' and in the isotropic phase '' at equilibrium in a polymer/solvent system vs. the axis ratio η. The dashed curves represent simple rods. The solid line represent a system of rigid molecules carrying random tails. The values were taken from ref. 46, reproduction with permission of the American Chemical Society. b) dependence of the order parameter s on $\bar{\eta}$ of a copolymer at selected values of the composition θ, ref. 55. Reproduction with permission of the American Chemical Society.

In contrast to the Flory-Matheson theory, Jonah *et al.* describe a neat liquid using, however, a more exact form of the orientational distribution function. Maier and Saupe as well as Flory and Ronca have derived a limiting value of the order parameter s at the anisotropic-isotropic phase

transition for $\bar{\eta} \rightarrow 0$, namely, $s_{limit} = 0.4291$. This agrees quite well with the value $s = 0.4347$ obtained from Figure 14b.

Figure 15 shows the dependence of the reduced transition temperature:

$$\hat{T} \equiv \frac{T_{aniso-iso}}{T^*} \tag{55}$$

and the order parameter as a function of $\bar{\eta}$ and $\bar{\theta}$.

Experimental values of $\bar{\eta} = 13.2$ Å for a longitudinal polymer liquid crystal were reported by Zachmann and co-workers.[59] Therefore, the values chosen for $\bar{\eta}$ in Figure 15 were chosen below and above this value. The figure shows that at large $\bar{\eta}$ small variations of the chain rigidity expressed by θ have large effects. Polydispersity will blunt sharp phase transitions as pointed out by Flory and Abe[34] and as shown by Matheson and Flory[46] it is the total number of rigid subchains which governs the thermodynamic behaviour of the polymer system rather than the allocation of the flexible subchains in the macromolecules.

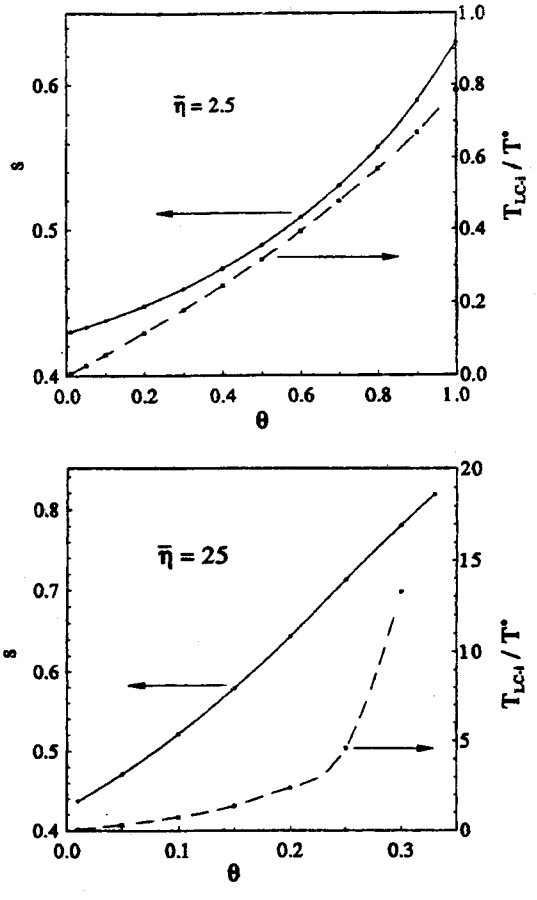

Figure 15. Dependence of the order parameter s and the anisotropic-isotropic (normalized) transition temperature $\hat{T}$ on the composition θ and the average length of the rigid subchains $\bar{\eta}$.[55] Reproduction with permission of The American Chemical Society.

At this point it is worth mentioning that the nature of the anisotropic (ordered) phase has not been specified. Matheson[47] has stressed the generality of the theory[46] and this also applies to the Jonah-Brostow-Hess approach.[55] Consequently, the ordered phase of Matheson[47] can be **any** type of liquid crystalline mesophase and is not restricted to nematic phases only.

$\bar{\eta} = 0$ describes the Maier-Saupe limit. $\theta = 0$ is a fully flexible polymer and the transition temperature that can be calculated is the temperature where the crystalline ordered phase coexists with the isotropic melt. With increasing concentration of the rigid subchains they act as impurities causing a melting point depression. At the limiting concentration (limit a situation is reached where there are just enough rigid subchains to form a second (anisotropic) phase. Experimentally, this phenomenon has been verified[58-61] as the occurrence of spherical islands[62] which can be deformed under external forces to form fibrillar, reinforcing structures in a matrix which itself is poor in ordered structures. The term θ_{limit} is closely related with Flory's average degree of flexibility[6] f - see equation 7. Matheson[47] has also derived a characteristic ratio C_∞ which describes the chain geometry and includes a measure of the average chain rigidity. This ratio also shows a limiting value that marks the border between the existence of anisotropic and isotropic phases.

The conditions around the anisotropic-isotropic phase equilibrium deserve closer inspection. This was done by Brostow and Walasek.[57] Eq. 51 gives no information about the stability of the ordered phase, and a criterion for the phase stability with respect to s is required.

Absence of external orienting fields provided, the Helmholtz function can be expanded in a

power series of s which is:

$$A = A_0 + \frac{1}{2}A_2 s^2 + \frac{1}{3}A_3 s^3 + O(s^4) \qquad (56)$$

Introducing the parameter X defined in eq. 58, the function $A(s)$ can be plotted at different constant parameters s, see Figure 16.

A_2 is positive, $A(s)$ has a mimimum at $s = 0$, which is a necessary condition for an isotropic equilibrium phase. The term s^3 does not vanish in an anisotropic phase since there is no symmetry relation between states with $s > 0$ and those with $s < 0$. For A_2 tending to zero and a non-zero, finite A_3 any isotropic phase becomes unstable compared with an ordered phase. If A_3 tends to zero an isotropic-anisotropic phase transition occurs. Using the Landau approach,[63] the coefficients of the reduced Helmholtz-function can be derived in the vicinity of $s = 0$. They are:

$$\widetilde{A}_2 = \left[1.56\,\bar{\eta}\theta\left(\frac{\theta}{\widetilde{T}}\right) + 100 - 20\left(\frac{\theta}{\widetilde{T}}\right)\right]\theta\left(\frac{\theta}{\widetilde{T}}\right)10^{-2} \qquad (57a)$$

$$\widetilde{A}_3 = \left[(1.95\,\theta + 8.20)\,\bar{\eta}\theta - 28.57\right]\theta\left(\frac{\theta}{\widetilde{T}}\right)^3 10^3 \qquad (57b)$$

The parameter:

$$X \equiv \frac{\theta}{\widetilde{T}} - \left(\frac{\theta}{\widetilde{T}}\right)_{LC-lim} \qquad (58)$$

denotes the difference of a certain state to the limiting state (= the lowest $\frac{\theta}{\widetilde{T}}$) where an ordered (liquid crystalline) phase can exist. The quotient is the already mentioned measure of the interaction energy ε. Now, equations 54 can be used again. They contain the physical parameters θ and $\widetilde{T}$ and the model parameters $\bar{y}$, $\bar{\eta}$, and s. For mathematical simplicity is substituted by γ using eq. 48 and 53. While the physical meaning of $\bar{\eta}$ and s is evident, this is not obvious for γ. A guess of the magnitude of $\bar{\eta}$ can be obtained from the molecular structure and/or experiment,[59] s can be measured. Now, for example, the Flory-Ronca algorithm[49,55] (γ is specified, s, $\bar{\eta}$ and $\widetilde{T}$ are calculated at a fixed composition θ) can be used to solve the set of equations 54 and $\bar{\eta}$ and $\widetilde{T}$ can be determined as functions of A_2 and A_3. Eq. 50 now obtains the form:

$$G_j(\gamma, S, A_2 A_3, \theta) = 0 \qquad (59)$$
$$j = 1, 2, 3$$

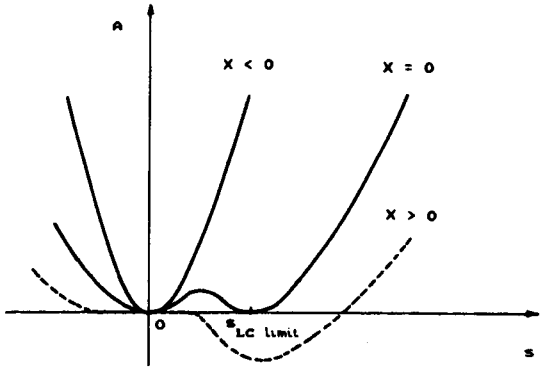

Figure 16. Qualitative behaviour of the Helmholtz Free Energy A as a function of the of the order parameter s calculated for different parameters X - see eq. 58. Reproduced from ref. 57 with permission of The American Chemical Society.

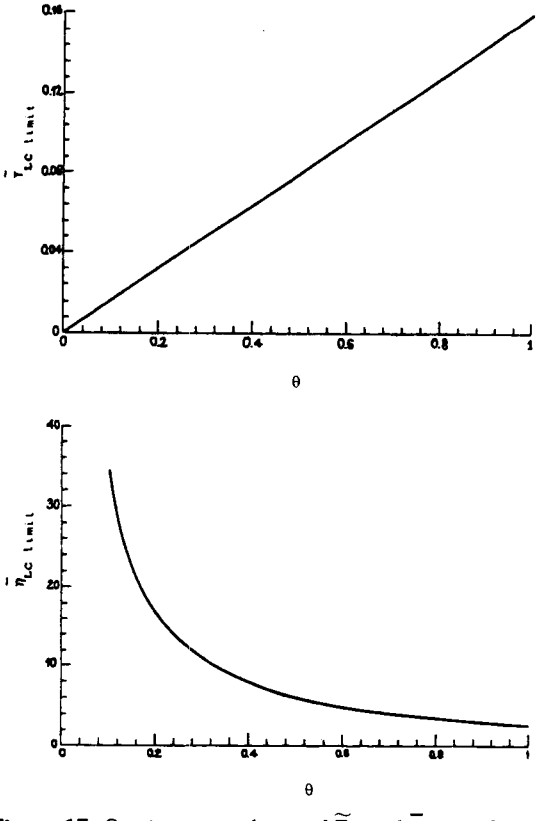

Figure 17. Coexistence conditions of $\widetilde{T}_{lim}$ and $\bar{\eta}_{lim}$ as a function of the composition of the polymer. After ref. 57 with permission of The American Chemical Society.

The conditions for the lowest composition θ_{lim} are given by $A_2 = A_3 = 0$ so that from eq. 57

$$\tilde{T}_{lim} = \frac{\theta(\theta+3.07)}{5(\theta=4.21)} \quad (60a)$$

and

$$\bar{\eta}_{lim} = \frac{14.65}{\theta(\theta=4.21)} \quad (60b)$$

are obtained. Now, it is the choice of θ that determines $\tilde{T}_{lim}$ and $\bar{\eta}_{lim}$ which are now variables depending on θ. The situation is shown in Figure 17.

If the concentration of the rigid subchains in a system is low the anisotropic interactions are low and therefore only a small amount of thermal energy is required to destabilize such an ordered system: $\tilde{T}_{lim}$ is small. The end of the coexistence of two phases for completely rigid systems ($\theta = 1$) is at $\tilde{T} = 0.16$ and there is only one isotropic phase stable beyond that temperature for rigid systems. There is also no coexistence between an anisotropic and an isotropic state possible below $\bar{\eta} = 2.81$. Even completely rigid polymers have to have at least this minimal value of $\bar{\eta}$ to obtain an anisotropic state. This result is in striking contrast to non-polymeric systems with relative strong interactions which do not require a minimum length of the rods[10,11,64] to obtain an anisotropic state.

Detailed mathematical analysis of the behaviour of s and X in stable anisotropic phases ($A_2 \rightarrow 0$) shows that there is a limiting value of s in the anisotropic phase $s_{lim,\,aniso} = 0.71$ ($\theta = 1$) and in the isotropic phase at $s_{lim,\,iso} = 0.73$, see Figure 18.

The corresponding value in the Maier-Saupe theory is $s = 0.44$. Maier-Saupe, however, describes monomolecular unconnected rigid rods ($\theta = 1$ and $\bar{\eta} = 1$) interacting by an anisotropy of optical transition moments. In systems of rods connected by flexible joints and random coil subchains that tend to maximise their conformational entropy the anisotropy of the rigid subchains has to be higher, and the repulsive interactions on contact are stronger in polymeric systems that can obtain a mesophase compared with a monomeric system. The fact that in the systems under consideration rigid subchains are connected by flexible parts results in a collective response of the rigid subchains on the orienting effects of a molecular mean field. As a consequence slim, aniso is increased. Experimental

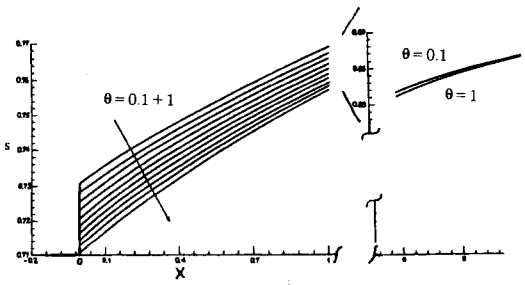

Figure 18. The function $s(X)_\theta$. The condition for a stable isotropic phase is $X < 0$, that for a stable anisotropic phase is $X > 0$, and $X = 0$ is valid at the phase transition. The limit values of s are indicated. s is only weakly depending on θ. The curves with different θ merge at high values of X, and the $s(X)$-dependence is almost negligible tending, however, to unity. There is a bifurcation point at $X = 0$. The right hand side of the diagram shows a magnification at higher values of X where the curves merge. Only the curve $\theta = 0.1$ and $\theta = 1$ are shown. Reproduced from ref. 57 with permission of The American Chemical Society.

results[65] and corresponding computer simulations[56] also find s closer to 0.72 than to the Maier-Saupe value of 0.44. At $X = 0$ there are two values of s, $s = 0$ and $s > 0$, indicating the coexistence of an anisotropic and an isotropic phase.

From a plot $\bar{\eta}$ vs. X - Figure 19 - the following conclusions can be drawn:

A small number of rigid subchains requires long subchains, especially if the interactions are week. A high $\bar{\eta}$ corresponds to a high transition tem-

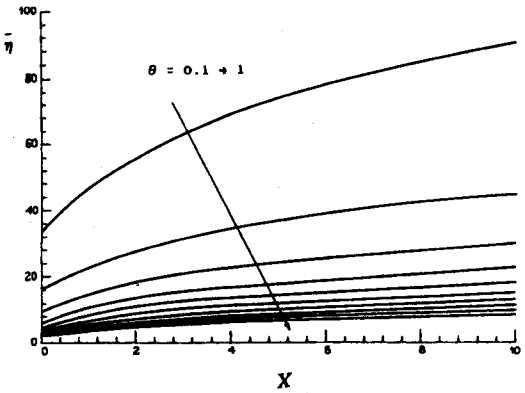

Figure 19. Dependence of the length of rigid subchains $\bar{\eta}$ on X (see eq. 58) with θ as parameter in anisotropic phases. Reproduced from ref. 57 with permission of The American Chemical Society.

perature since $\bar{\eta} \propto T$ as can be derived from eq. 58 and 36 and the fact that $\bar{\eta} = x$. The influence of polydispersity on the phase behaviour is presently subject of further investigations.

Brostow and Walasek used a non-lattice approach[52] to look deeper into details of the phase transitions semirigid polymers can undergo. Figure 20 explains the chain model used in this approach.

The distribution function ρ of the interacting rigid subchains is given by the Gibbs function, for flexible subchains ρ is given by a Dirac delta function, see for example Chandrasekhar,[66] Ishihara,[67] Flory[68] and Grosberg and Khokhlov.[69] The two subchains are not assumed to be homeomorphic with respect to each other.

The Helmholtz free energy A is given by:

$$A = U - T \cdot S \tag{61}$$

The energy U of the system is given by:

$$U = -\frac{kTu_h s^2}{2} \tag{62}$$

from a multipole expansion of uniaxially symmetrical electron clouds interactions (restricted to the quadrupole term) induced in the rigid subchains. The positive constant uh is a measure of the interacting forces between the rigid subchains according to Flory.[70,71] s is the order parameter as defined in eq. 35, which actually is the average of the average second Legendre polynomal $<P_{2j}>$ over all rigid subchains N_h:

$$s = \frac{1}{N_h} \sum_{j=1}^{N_h} <P_{2j}> \tag{63}$$

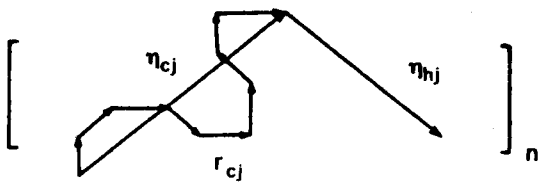

Figure 20. Shown is the j[th] constitutional repeating unit (CRU) of a semiflexible polymer molecule comprising alternating flexible (left) and rigid subchains (right). The whole macromolecule contains n CRUs. $\mathbf{r}_{cj}$ is a segment vector with the length l equal to unity for all of them. η_{cj} and η_{hj} are the end to end vectors of the flexible and the rod-like subchain, respectively. Reproduced from ref. 52 with permission of The American Institute of Physics.

The average $<P_{2j}>$ is calculated from the distribution function. The entropy of the system is given by:

$$S = S_h + S_c = k \ln \int \cdots \int \exp\left[\frac{-u\hat{\eta}_h}{kT}\right] \times p(\hat{\eta}_h, \Lambda^{-1}, \hat{r}) \times d\hat{\eta}_h \, d(\Lambda^{-1}, \hat{r}) + \frac{1}{T} <u(\hat{\eta}_h)> + k <\ln p(\hat{\eta}_h, \hat{r})> \tag{64}$$

"^" denotes the set of vectors of a subchain, p is the statistical probability of the system with the distribution function ρ so that the entropy S is given by:

$$S = k \ln p = -k \ln <\rho> \tag{64a}$$

Λ^{-1} is the inverse matrix of the deformation gradient matrix Λ. It has to be introduced because Flory observed that averaging of thermodynamic functions with respect to their end-to-end distance vectors r requires information about the symmetry of the integration space.[72] Details of the extensive derivative are given in ref. 52.

After integration the uniparticle Helmholtz function is given by:

$$\tilde{A}\, kT \left\{ \frac{u_h s(s+1)}{2} - \ln \int_0^1 \exp\left[\frac{3u_h s z^2}{2}\right] dz + \frac{3K}{2<n>} \times \left[\frac{(\Lambda_x - 1)^2(1 - <z^2>)}{2} + \frac{(\Lambda_y - 1)^2(1 - <z^2>)}{2} + (\Lambda_z - 1)^2(1 - <z^2>)\right] + const \right\} \tag{65}$$

If chains are connected with other chains via their ends, the integration has to be modified with respect to the type of the connection. The integration can become rather difficult depending on the topology of the system. "<...>" always identifies analytical averages over all chains, so that $<z^2>$ is the second moment and (is defined by:

$$K = <\frac{n <\eta_h^2>_{l,int}}{r_c}>_l = <\frac{<\eta_h^2>_{l,int}}{<\eta_c>_{l,int}}>_l \tag{65a}$$

For $\kappa = 0$ or $<n> \rightarrow \infty$ eq. 65 reduces to the result given by Maier and Saupe for non-polymeric liquid crystals.[10,11] Now, $\tilde{A}$ can be written as a function of the order parameter s and the conditions for thermodynamic equilibrium can be applied. Self-consistency of the molecular field is

given by the condition that $\widetilde{A}(s)$ has to show a global minimum in each coexisting phase. The function $\widetilde{A}(s) - \widetilde{A}(0)$ is plotted for various conditions in Figure 21.

The phase diagrams can be discussed in terms of the energy u_h. At any condition $u_h < 4.54$ there is only one global minimum at $s = 0$, which means that only the isotropic phase is stable. This is valid for monomeric and for polymeric systems, Figure 21a. If $u_h > 4.54$ phases with $s = 0$, $s > 0$ (e. g.: nematic, N, or smectic, S) and $S < 0$ (e. g.: S*- or N*-phases, see Figure 13) are possible. This behaviour is a simple result of the theory outlined above and does not require any additional assumptions. Previous theories, for example Varichon and Ten Bosch[53,54] had to introduce additional molecular mechanisms to describe states with $s < 0$. These different phases can coexist and even form triphasic equilibria, for example Figure 21c. The phase transitions $s = 0 \rightarrow s < 0$, $s = 0 \rightarrow s > 0$ and $s < 0 \rightarrow s < 0$ are all of first order, Ehrenfest[27] and Landau,[65] since s shows a discontinuity (step) at the transition, just as the entropy S and the volume. An example for this behaviour will be shown later, Figure 30, at the occasion of the more complex example of a polymer network which shows essentially the same effects. The phase structure can be visualized in a $(u_h)^{-1}$ vs. κ diagram, see Figure 22.

Compared with Maier-Saupe's mean field approach and the Flory theory, respectivly, there is:

$$u = \underbrace{\frac{u'}{kT}}_{\text{Maier-Saupe}} = \underbrace{\frac{\theta \bar{\eta}_h}{T^*}}_{\text{Flory}} \qquad (66)$$

The fundamental distribution ρ from which the Brostow-Walasek treatment starts depends on the chain end-to-end distance vectors and the the interactions between the rigid subchains, and in its general form it is valid for polydisperse systems and arbitrary topology of chain connections, hence also includes networks, as will be addressed later. Consequently, the same is true for the ther-

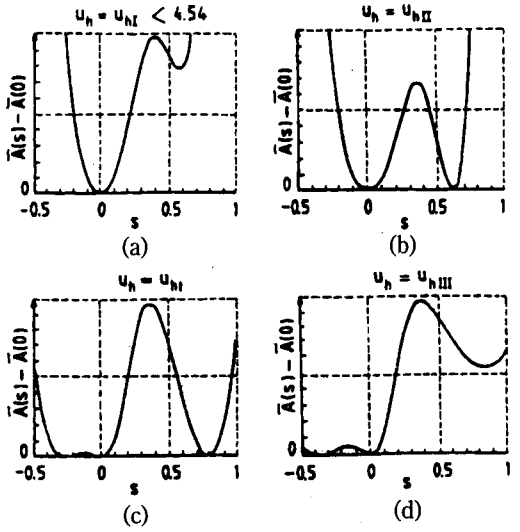

Figure 21. Typical behaviour of the function $\widetilde{A}(s) - \widetilde{A}(0)$ vs. s for semi-rigid polymers with uh as parameter. a) stable isotropic phase in a monomeric respectively polymeric system. b) biphasic equilibrium isotropic - N (or S). c) triphasic equilibrium N* (or S*) - isotropic - N (or S). d) biphasic equilibrium N* (or S*) - N (or S). Calculated in the limit of a molecular mean field and with a Gaussian distribution of the flexible chains. Further explanation see text. Reproduced after ref. 52 with permission of The American Institute of Physics.

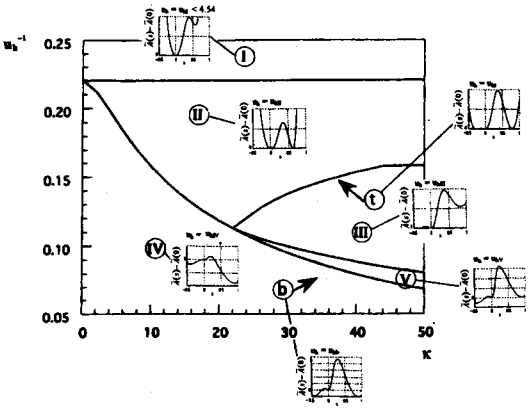

Figure 22. Phase diagram in terms of $(u_h)^{-1}$ and κ for a semi-rigid polymer system with mesophases. The average number of subchains per chain <n> was 10. The shape of the diagram, does not change with <n>, although the scaling differs. The small diagrams were partly taken from Figure21. **Area I:** $u_h < 4.54$, the system shows one equilibrium isotropic phase. **Area II - V:** $u_h < 4.54$ in particular **Area II:** the system is in a biphasic equilibrium iso - N (or S). **Phase III:** biphasic equilibrium i - N* (or S*). **Phase IV:** one nematic (N) or smectic phase (S). **Phases V:** one ordered phase N* or S* **line b:** biphasic equilibrium N* - N or S* - S. **line t:** triphasic equilibrium N* (or S*) - iso - N (or S). After ref. 52 with permission of The American Institute of Physics.

modynamic functions derived from ρ. The behaviour of these semi-rigid systems can be described by the competition between uniaxial *energetic effects* that orient the rigid structures and the predominantly *entropic effects* contributed by the flexible structures. Again there are the two competitors ΔS and ΔU (or ΔH) the interplay of which governs the entire physics of polymeric systems as a general principle. Kricheldorf and coworkers[73-77] found basing on a large number of longitudinal, aromatic polyesters that the formation of mesophases is favoured by large bond angles ($\approx 130°$). They judge the influence of the bond angle as important as the rigidity of the subchains.

Subsequent to ref. 55, Blonski, Brostow, Jonah and Hess[56] made use of the Matheson-Flory[46] theory with the orientational contribution represented by the Flory-Irvine term[58] in the distribution function and calculated-expanding their earlier work[55]-the phase diagram of ternary systems comprising polymers consisting of solvent (1), semi-flexible polymer (2), and coil polymer (3). The semi-flexible polymer is of the same type as modelled in Figure 10. Using the same procedure as described above[55] they arrive at the equilibrium condition in terms of the chemical potential $\mu_i' = \mu_i''$ which yields for the three components:
solvent (1)

$$\ln\left(\frac{\upsilon'_1}{\upsilon''_1}\right)+(\upsilon'_p-\upsilon''_p)\left(1-\frac{1}{r}\right)+\chi(\upsilon'^2_p-\upsilon''^2_p) = \ln(1-Q)+Q \tag{67a}$$

semi-rigid polymer (2)

$$\frac{1}{r_2}\ln\left(\frac{\upsilon'_2}{\upsilon''_2}\right)+(\upsilon'_p-\upsilon''_p)\left(1-\frac{1}{r}\right)+\chi(\upsilon'^2_s-\upsilon''^2_s)= \left[1-\theta\left(1-\frac{4f_2}{\pi f_1}\right)\right]\ln(1-Q) \tag{67b}$$

coil polymer (3)

$$\frac{1}{r_3}\ln\left(\frac{\upsilon'_3}{\upsilon''_3}\right)+(\upsilon'_p-\upsilon''_p)\left(1-\frac{1}{r}\right)+\chi(\upsilon'^2_1-\upsilon''^2_1) = \ln(1-Q)+Q \tag{67c}$$

with:

$$\upsilon_p \equiv \upsilon_2+\upsilon_3 \tag{68}$$

$$Q=\theta\upsilon'_2\left(1-\frac{4f_2}{\pi f_1}\right) \tag{69}$$

$$f_j=\int_0^{\frac{\pi}{2}} \sin^j\Psi\exp\left[-\gamma\sin\Psi-\frac{3}{2}\theta\upsilon'_2 s\,\tilde{T}^{-1}\sin^2\Psi\right]d\Psi \tag{70}$$

$$j=1,2,3$$

Eqs. 69 and 70 differ from eqs. 48 and 52 only by the factor υ'_2, the other symbols are already familiar. Details of the numeric calculation are given in ref. 55 and 56. The introduction of the "anisotropic-isotropic transition volume fraction" by Figari and Costa[78] facilitates the calculation of ternary phase diagrams significantly. Physically this volume fraction is the smallest concentration that can cause anisotropic phases. It is a quantitative measure of the tendency of a polymer to extend its peculiar anisotropy to the other components of a given ternary system.

Sign and magnitude of the Flory-Huggins-Staverman-interaction parameter θ were found to be of minor importance as proved by Figure 23.

The influence of variation of the characteristic temperature T^* and θ were studied while χ was set to zero, which is the athermal case. The results are shown in Figure 24 and 25.

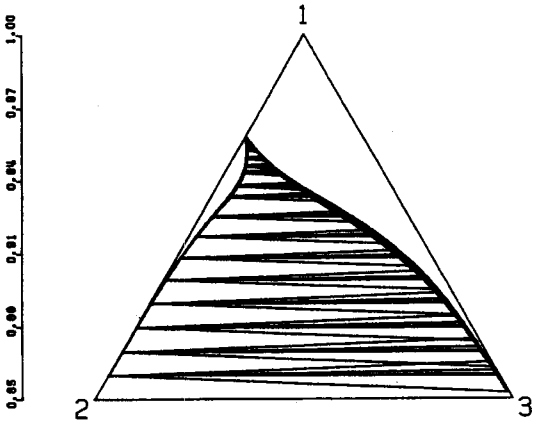

Figure 23. The influence of the Flory-Huggins-Staverman-interaction parameter χ on the shape of a ternary phase diagram comprising solvent (1), semi-rigid polymer (2), and coil polymer (3). The parameters are: $\theta=0.35$, $r_2=600$, $r_3=1200$, $T^*=300$K and $T=295$ K. The diagram was calculated for $\chi=-10$, -1, 0, 1 and 10. Reproduced from ref. 56 with permission of The American Chemical Society.

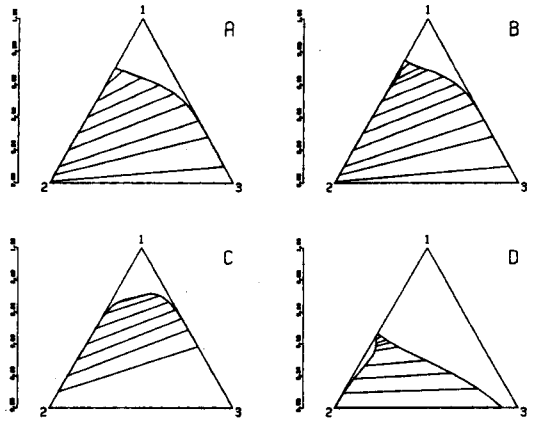

Figure 24. Phase diagram for the ternary system $r_2 = r_3 = \bar{r} = 20$ (corresponds to x_2 and x_3 in ref. 38, see also Figure 2 there), $T = 300$ K. A) $T^* = 50$ K, $\theta = 1$ B) $T^* = 100$ K, $\theta = 1$ C) $T^* = 200$, $\theta = 1$ D) $T^* = 100$ K, $\theta = 0.7$ Reproduced from ref. 56 with permission of The American Chemical Society.

Figure 24 A) and B) correspond to completely rigid rods since $\theta = 1$. A) is quite similar to Figure 2 in ref. 38. B) Changing, however, the characteristic temperature T^*, which represents the interaction between rigid subchains, the miscibility gap becomes larger indicating a lower solubility of the semi-flexible polymer in the solvent compared with flexible polymer. There is not much of the semi-rigid polymer in the isotropic phase. A small area indicating an anisotropic, ordered phase containing more component 2 than 3 opens on the left side of the triangle. The critical point is localized in the tip in the left part, the tie lines vanish there. C) Increasing the interaction of the rigid parts increases the solubility of the semi-rigid polymer in the solvent shifting the critical point accordingly. As has been shown by Brostow and Sochanski,[79] T^* of a system is actually a function of all individual T_i^*. Hence, the behaviour of the ternary diagram on variation of T^* is a response of the mutual interactions of the components. Finally, D) shows the effect of decreasing the chain rigidity: while there were completely rigid rods treated in the examples A)-C), the flexibility has been increased in example D) by changing only the fraction of rigid subchains from $\theta = 1$ to $\theta = 0.7$. As expected, the homogeneous isotropic region grows, and more of the flexible polymer becomes soluble in the isotropic phase. Again, the miscibility of the semi-rigid polymer shows a second window at higher concentrations. It can be concluded from these examples that it is the strength of the interactions (i. e.: T^*) that determines the type of behaviour of the system, and that the extend of flexibility (i. e.: θ) influences the area of the miscibility gap rather than its shape.

Figure 25 shows the experimental results[67] obtained with a system consisting of $CHCl_3$ (component 1), poly(ethylenetherephthalate-co-*ran*-*p*-hydroxybenzoate) (component 2), and polycarbonate (component 3) compared with the ternary phase diagram as calculated.[56]

The general trend shown in Figure 24b and d is reflected by the experimental values, the cusp, however, is only indicated by the experimental values which were obtained from cloud point measurements, the tie lines of the corresponding phase compositions, however, had not been experimentally determined. Since θ is close to the limiting value, the experimental technique was relatively insensitive and the fact that the polymers were polydisperse the results are not in contradiction with theory. Description of the system according to Flory assuming completely rigid rods was not successful in this case.

Stronger support for Blonski's approach was delivered by Marsano and co-workers,[80] who in

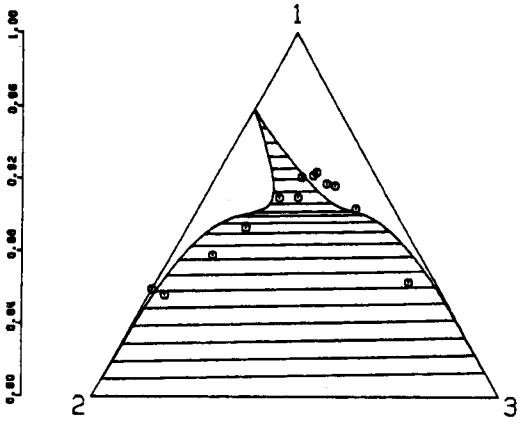

Figure 25. Experimental results and calculated ternary phase diagram. The parameters are: $\theta = 0.27$, $\eta = 162$, $T = 295$K, $T^* = 600$K, $r_2 = 600$, $r_3 = 1200 \rightarrow \bar{r} = 900$. Reproduced from ref. 56 with permission of The American Chemical Society.

fact unequivocally observed an anisotropic phase that did not completely exclude coil polymers from the anisotropic phase of a ternary system. Their system consisted of the solvent dimethylacetamid (DMA) + LiCl (component 1), the rigid poly(*p*-benzamide) - (PBA) - (component 2), and the flexible component 3, poly(2-phenylene-5-benzimidazole - isophthalamide) - (PABI). Figures 26 and 27 show calculated phase diagrams and experimental values.

While the anisotropic phase accepts a maximum of about 5% (v/v) of the coil polymer with the low molar mass, the high molar mass coils are completely excluded confirming the predictions of Blonsky.[56] The experimental tie lines (conodes) are steeper than the theoretical ones which means a less pronounced segregation of the components, caused probably by non-zero χ-parameters and polydispersity of the polymers. Figure 28, on the contrary, shows the phase diagram of a system that already shows phase separation in the isotropic state. The features of such a phase diagram are completely different from those described above.

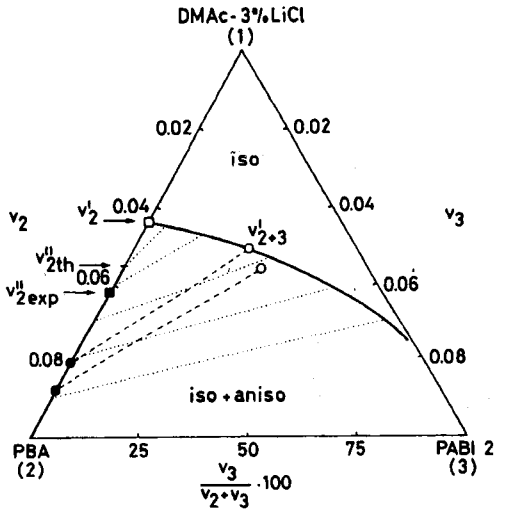

Figure 26. Ternary phase diagram of the system (DMA + LiCl) + PBA + PABI at 20°C. M_w (PBA) = 11,800 g/mol, M_w (PABI) = 12,400 g/mol. The open circles correspond to the composition of the isotropic phase, the full circles correspond to the of the conjugated anisotropic phase. Reproduced from ref. 82 with permission of Huethig and Wepf.

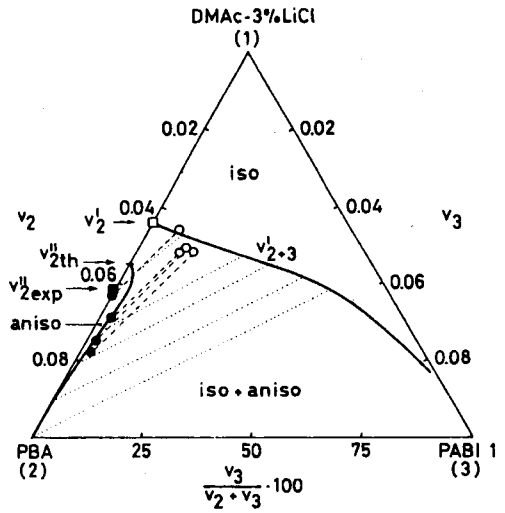

Figure 27. Ternary phase diagram of the system (DMA + LiCl) + PBA + PABI at 20°C. M_w (PBA) = 54,000 g/mol, M_w(PABI) = 12,400 g/mol. The open circles correspond to the composition of the isotropic phase, the full circles correspond to the of the conjugated anisotropic phase. Reproduced from ref. 82 with permission of Huethig and Wepf.

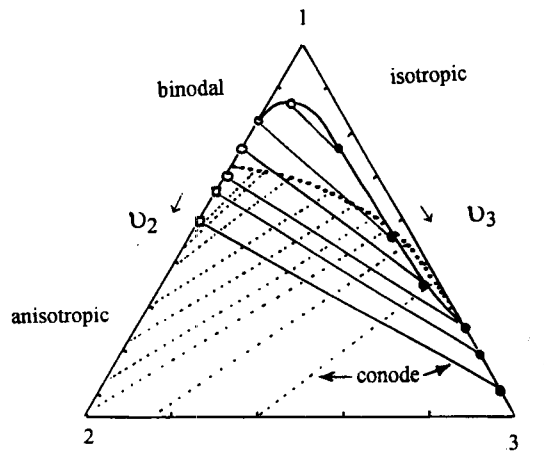

Figure 28. Phase diagram of the system: dimethylacetamide + LiCl (component 1), cellulose (component 2), and cellulose diacetate (component 3) at 20°C. The circles designate isotropic phases, the squares an anisotropic phase. The tie lines combine the conjugated phases. The phase diagram calculated according to Flory[38] is indicated by dotted lines. The slope of the tie lines and the shape of the experimental results are entirely different from the calculated diagram, not because of invalidity of the theory but because there is an incompatibility of the polymers already in the isotropic state. Redrawn using values of Marsano *et al.*[44] with permission of The American Chemical Society.

Non-linear Molecules

Flory's lattice calculations[38] have shown that strong repulsions between rod-like molecules and flexible coil-type molecules caused by entropic effects allow only small concentrations of rigid chains in an isotropic phase, and that the anisotropic phase almost completely excludes flexible chains. The mutual miscibility can be increased by attaching flexible side chains the rigid polymer molecule. Although such modifications are suitable to increase the miscibility of binary and ternary systems significantly, their practical application as reinforcing components may be limited since the diameter of such a modified molecule increases, hence decreasing its aspect ratio. The problem has been studied practically and theoretically by Ballauff.[81-83] The polymer molecules are placed on the lattice as described earlier. Soft interactions between rod-type subchains and solvent $\chi(1, 2)$, coil-type subchain and solvent $\chi(1, 3)$, and rod-type subchain/coil-type subchain $\chi(2, 3)$ were introduced which combine to:

$$\chi_1 = \chi_{(1,2)} + \frac{zm}{x}\chi_{(1,3)} \tag{71}$$

$$\chi_2 = \frac{zm}{x}\chi_{(2,3)} \tag{72}$$

where 1 denotes the solvent, 2 the rigid rod, and 3 the coil molecule.

Following the procedure given by Flory and Ronca[49] the chemical potentials in the anisotropic phase are given by:

$$(\mu_1 - \mu_{01})' = RT\left\{\ln v'_1 + v'_s + v'_x\left(1-\frac{1}{x}\right) + v'_x\left[v'_x + v'_s\chi_1 - \frac{v'_x}{x}\frac{zm}{x}\chi_2\right]\right\} \tag{73}$$

$$(\mu_x - \mu_{0x})' = RT\left[\ln\frac{v'_x}{x} + f_1 + f_1\left(v_x + \frac{v'_x}{x}\right) - \ln\sigma + \left(1-v'_x\frac{f_1}{x}\right)\left(v'_x\chi_1 + v'_x\frac{zm}{x}\chi_1\right)\right] \tag{74}$$

The chemical potentials in the isotropic phase are given by:

$$(\mu_1 - \mu_{01})'' = RT\left\{\ln v''_1 + v''_1 + \frac{v'_1}{x}(\bar{y}-1) + \frac{2}{\bar{y}} + v''_1\left[(v''_1 + v''_x)\chi_1 - \frac{v''_1}{x}\frac{zm}{x}\chi_2\right]\right\} \tag{75}$$

$$(\mu_x - \mu_{0x})'' = RT\left[\ln\frac{v''_x}{x} - f_1\left(v''_1 + \frac{v''_x}{x}\right) + f_1 - v''_x\left(1-\frac{\bar{y}}{x}\right) + \frac{2zm}{\bar{y}} + 2(1-\ln\bar{y}) - \ln\frac{\sigma}{x^2} - 2\ln\left(\frac{\pi e}{8}\right) + \left(1-v''_x\frac{f_1}{x}\right)\left(v''_1 x\chi_1 v''_x\frac{zm}{x}\chi_2\right)\right] \tag{76}$$

The definitions used earlier - eq. 11-15, 40 and the general definition of f_i eq. 39 are still valid, the terms σ and $2\ln\left(\frac{\pi e}{8}\right)$ are negligible. Figure 29 shows the calculated phase diagram of these modified rod-like molecules.

The addition of flexible side chains changes the properties of the system significantly, even at low concentrations of the side chains: the area in the phase diagram where nematic phases coexist decreases. For the chosen example, this region becomes unstable for $zm > 4$. The value of the interaction parameter at the critical point and at the triple point increases upon adding side chains to the rods. The miscibility gap decreases, and the biphasic regime appears at lower temperatures. Experimental results from lyotropic polypeptides, as for example poly(γ-benzyl glutamate), are in qualitative agreement with the theory, however, intra-and intermolecular interactions require further investigation concerning their contribution to the phase behaviour.

Another approach was followed by Wendorff and coworkers[84] investigating rigid rods with rigid side chains. Gallenkamp[85] has undertaken lattice calculations on these types of rigid branched molecules. By introducing a second order parameter it was possible to describe the behaviour of these three-dimensional structures. The solubility in binary as well as in ternary systems was unexpectedly high and a compatibilization is predicted not only in the isotropic state but also in the anisotropic state.[86,86]

The investigation of systems consisting of semi-rigid macromolecules with flexible side chains localized at the spacers[87,88] connecting the rigid subchains is presently under investigation.[89]

In a recent work, Brostow, Hibner and Walasek[90] have extended the theory presented in ref. 52 and have treated connected chains, which here means non-linear macromolecules

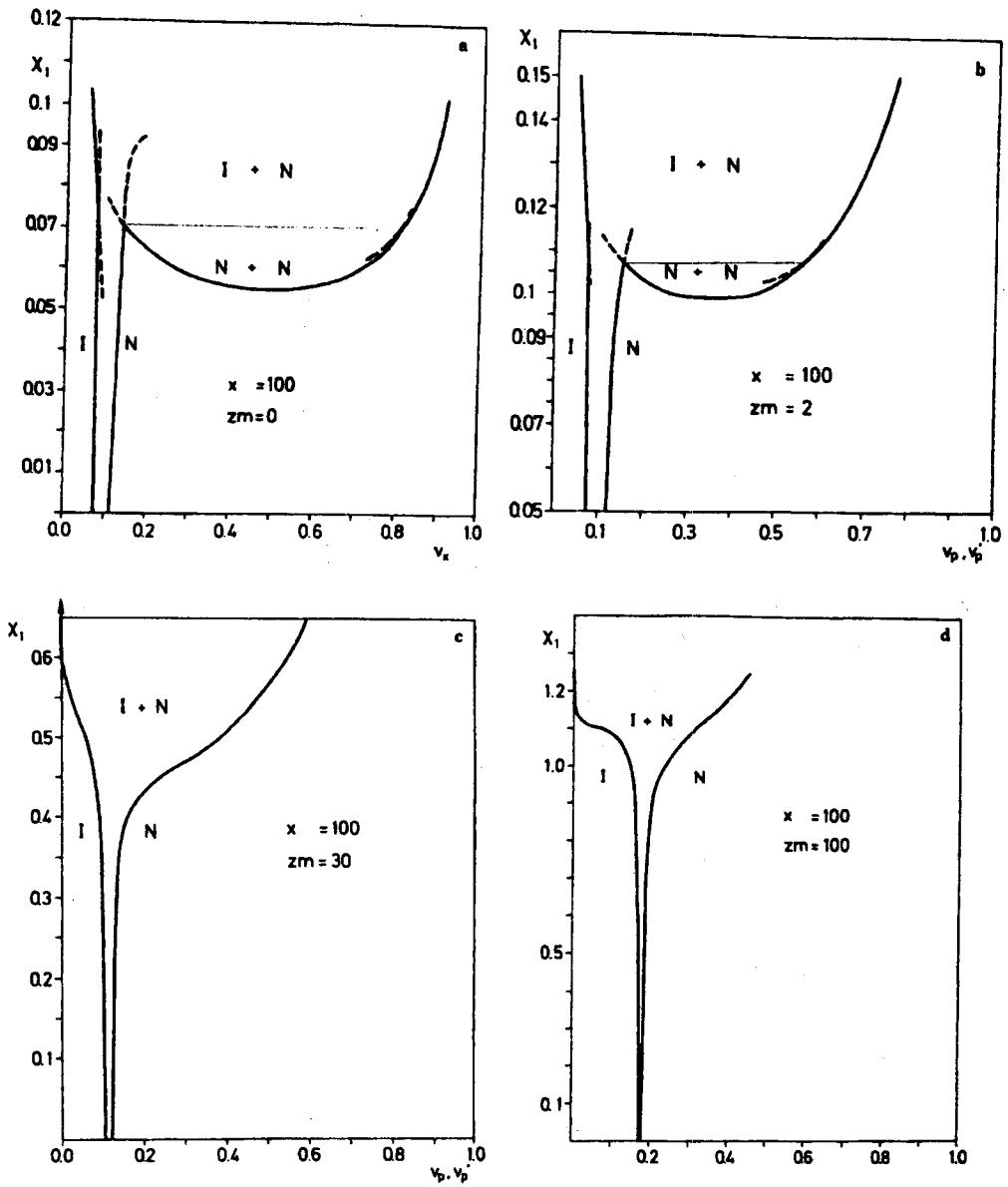

Figure 29. Phase diagram of side chain modified rigid rods in a low molar mass solvent (index 1). x denotes the aspect ratio of the rigid backbone (index 2), z is the number of the side chains (index 2) per rigid core and m is the number of the segments per side chain, as defined earlier. The solvent quality is measured by the Flory-Huggins-Staverman-interaction parameter χ_1, which depends on temperature and concentration. υ_p and υ_x are the volume fractions of the total polymer and its rigid core, respectively. After ref. 84, reproduced with permission of The American Chemical Society.

such as networks, in some more detail. They introduce the coefficient A_c:

$$A_c = \frac{<r^2>_{con}}{<r^2>_{uncon}} \tag{77}$$

since a connection of chains via their ends forming a network causes a reduction of the number of independent end-to-end vectors r compared with the very same system but with the chains unconnected. This reduction now causes a contraction of the chain end-to-end distances[91,92]

Following ref. 52 they derive the Helmholtz

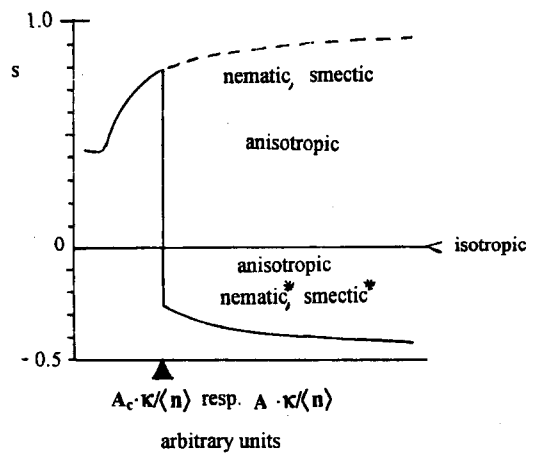

Figure 30. The function $\widetilde{A}(s)$ with a first order phase transition.[92]

function corresponding to eq. 65 and finally arrive at the equation of consistency of the molecular field as described earlier.

$$\widetilde{A} = kT\left\{\frac{u_h s(s+1)}{2} - \ln\int_0^1 \exp\left[\frac{3u_h s z^2}{2}\right] dz + \frac{3A_c K}{2\langle n\rangle} \times \left[\frac{(\Lambda_x - 1)^2(1-\langle z^2\rangle)}{2} + \frac{(\Lambda_y - 1)^2(1-\langle z^2\rangle)}{2} + (\Lambda_z - 1)^2\langle z^2\rangle\right] + const\right\} \quad (78)$$

The minima of $\widetilde{A}(s)$ are analyzed and the global minima are identified. Eq. 65 and eq. (78) only differs in the term A_c. The phase behaviour of these crosslinked systems can be visualized as before, see Figure 22, except that s is plotted vs. $A_c \cdot \kappa$. The shape of the phase diagram is practically the same, and the phase transitions are first order as reported earlier. Figure 30 shows examples of different phase transitions, all are first order transitions[27,65] with a discontinuity in the first derivative of $\widetilde{A}(s)$.

Finally, it has to be mentioned that the theoretical description of discotic polymers recently has been attacked by Moscicki.[93]

Acknowledgement. The author is greatly indebted the Polymer Society of Korea and the Deutsche Forschungsgemeinschaft for financial support. Special thanks are due to Janusz Walasek, Technical University of Radom, Poland, Werner Borchard, Gerhard-Mercator-University Duisburg, Germany, Witold Brostow, University of North Texas, Denton, U. S. A., and Jung-Il Jin, Korean University, Seoul, Korea, for fruitful discussions, encouragement and support.

References

(1) W. Brostow (ed.), *Performance of Plastics*, Hanser, Mü nchen, in press.
(2) A. H. Fawcett (ed.), *High Value Polymers*, The Royal Society of Chemistry, Cambridge, 1991.
(3) A. Ciferri and I. M. Ward (eds.), *Ultra-High Modulus Polymers*, Applied Science Publishers Ltd., Barking, Essex, England, 1979.
(4) A. E. Zachariades and R. S. Porter (eds.), *The Strength and Stiffness of Polymers*, Plastics Engineering Vol. IV, Marcel Dekker Inc., Basel, New York, 1983.
(5) W. Brostow, *Science of Materials*, John Wiley & Sons Inc., New York, 1979.
(6) P. J. Flory, *Proc. Roy. Soc.* (London), **A 234**, 60 (1956).
(7) P. J. Flory, *Proc. Roy. Soc.* (London), **A 234**, 73 (1956).
(8) L. Onsager. *Ann. N. Y. Acad. Sci.*, **51**, 627 (1949).
(9) A. Ishihara. *J. Chem. Phys.*, **19**, 1142 (1951).
(10) W. Maier and A. Saupe, *Z. f. Naturforschung*, **14a**, 882 (1959).
(11) W. Maier and A. Saupe, *Z. f. Naturforschung*, **15a**, 287 (1960).
(12) W. Brostow, *Polymer*, **31**, 979 (1979).
(13) M. Hess in *Performance of Plastics*, W. Brostow (ed.), Hanser, München, in press.
(14) E. A. Guggenheim, *Mixtures*, Clarendon Press, Oxford, England, 1952.
(15) E. A. Guggenheim, *Application of Statistical Mechanics*, Clarendon Press, Oxford, England, 1966.
(16) P. J. Flory, *J. Phys. Chem.*, **10**, 51 (1942).
(17) M. L. Huggins, *Ann. N. Y. Acad. Sci.*, **41**, 1 (1942).
(18) E.-A. Guggenheim, *Boltzmann's Distribution Law*, North Holland, Amsterdam, 1955.
(19) E. Schringer, *Statistical Thermodynamics*, Cambridge University Press, Cambridge, 1948.
(20) P. G. de Gennes and C. R. Hebd, *Seances Acad. Sci.*, **B 281**, 101 (1975).
(21) P. J. Jarry and L. J. Monnerie, *J. Polym. Sci. Phys.*, **16**, 443 (1978).
(22) J. Walasek, *J. Polym. Sci.*, **26**, 1907 (1988).
(23) J. Walasek, *J. Polym. Sci.*, **28**, 1075 (1990).
(24) J. Walasek, *J. Polym. Sci.*, **28**, 2473 (1990).
(25) P. J. Flory, *Disc. Faraday Soc.*, **49**, 7 (1970).
(26) P. J. Flory, *J. Macromol. Sci.: Phys. Ed.*, **B 12**, 1 (1976).
(27) P. Ehrenfest, *Proc. Kon. Acad. Wetensch, (Amsterdam),*

36, 153 (1933).
(28) J. Hermans, *J. Coll. Sci.*, **17**, 638 (1962).
(29) E. L. Wee and W. G. Miller, *J. Phys. Chem.*, **75**, 1446 (1971).
(30) P. W. Morgan, *Macromolecules*, **10**, 1381, 1390, 1396 (1977).
(31) S. P. Papkov, V. G. Kalichikhin, and D. Kalmykova, *J. Polym. Sci. Phys.*, **12**, 1753 (1974).
(32) J. P. Straley, *Mol. Cryst., Liq. Cryst.*, **22**, 333 (1973).
(33) P. J. Flory and G. Ronca, *Mol. Cryst., Liq. Cryst.*, **54**, 289 (1979).
(34) P. J. Flory and A. Abe, *Macromolecules*, **11**, 1119 (1978).
(35) A. Abe and P. J. Flory, *Macromolecules*, **11**, 1122 (1978).
(36) P. J. Flory and R. S. Frost, *Macromolecules*, **11**, 1126 (1978).
(37) R. S. Frost and P. J. Flory, *Macromolecules*, **11**, 1134 (1978).
(38) P. J. Flory, *Macromolecules*, **11**, 1138 (1978).
(39) P. J. Flory, *Macromolecules*, **11**, 1141 (1978).
(40) S. M. Aharoni, *Macromolecules*, **12**, 94, 271, 537 (1979).
(41) S. M. Aharoni, *Polymer*, **21**, 21 (1980).
(42) W. F. Hwang, D. R. Wiff, and C. Verschoore, *Polym. Eng. Sci.*, **23**, 789 (1983).
(43) E. Bianchi, A. Ciferri, and A. Tealdi, *Macromolecules*, **15**, 1268 (1982).
(44) E. Marsano, E. Bianchi, A. Ciferri, G. Ramis, and A. Tealdi, *Macromolecules*, **19**, 626 (1986).
(45) E. Marsano, M. Tamagno, E. Bianchi, M. Terbojevich, and A. Cosani, *Polymers for Advanced Technology*, **4**, 25 (1992).
(46) R. R. Matheson and P. J. Flory, *Macromolecules*, **14**, 954 (1981).
(47) R. R. Matheson, *Macromolecules*, **19**, 1286 (1986).
(48) P. J. Flory and R. R. Matheson, *J. Chem. Phys.*, **88**, 6606 (1984).
(49) P. J. Flory and G. Ronca, *Mol. Cryst. Liq. Cryst.*, **54**, 311 (1979).
(50) P. H. Hermans and P. Platzek, *Kolloid Z.*, **88**, 68 (1939).
(51) J. J. Hermans, P. H. Hermans, D. Vermaas, and A. Weidinger, *Rec. Trav. Chim. Pays-Bas*, **65**, 427 (1946).
(52) W. Brostow and J. Walasek, *J. Chem. Phys.*, **105**, 4367 (1996).
(53) L. Varichon and A. Ten Bosch, *Liq. Cryst.*, **14**, 1635 (1993).
(54) L. Varichon and A. J. Ten Bosch, *J. Chem. Phys.*, **100**, 1708 (1994).
(55) D. A. Jonah, W. Brostow, and M. Hess, *Macromolecules*, **26**, 76 (1993).
(56) S. Blonski, W. Brostow, D. A. Jonah, and M. Hess, *Macromolecules*, **26**, 84 (1993).
(57) W. Brostow and J. Walasek, *Macromolecules*, **27**, 2923 (1994).
(58) P. J. Flory and P. A. Irvine, *J. Chem. Soc. Faraday Trans.*, **1**, 80, 1807 (1984).
(59) E. Olbrich, D. Chen, H. G. Zachmann, and P. Lindner, *Macromolecules*, **24**, 4364 (1991).
(60) J. Menczel and B. J. Wunderlich, *J. Polym. Sci. Phys.*, **18**, 1433 (1980).
(61) M. Uzman, K. Knpast, and J. Springer, *J. Makromol. Chem.*, **190**, 3185 (1988).
(62) M. Kwiatkowski and G. Hinrichsen, *J. Mater. Sci.*, **25**, 1548 (1990).
(63) W. Brostow and M. Hess, *Mater. Res. Soc. Symp.*, **255**, 57 (1989).
(64) W. Brostow, T. S. Dziemianowicz, J. Romanski, and W. Werber, *Polym. Eng. Sci.*, **28**, 785 (1988).
(65) L. D. Landau, *Collected Papers*, D. ter Haar (ed.), Gordon & Breach, New York, 1965, pp 193.
(66) P. G. De Gennes, *Physics of Liquid Crystals*, Clarendon Press, Oxford, U. K., 1974.
(67) F. Schubert, K. Friedrich, M. Hess, and R. Kosfeld, *Mol. Cryst. Liq. Cryst.*, **155**, 477 (1988).
(68) S. Chandrasekhar, *Rev. Mod. Phys.*, **15**, 1 (1943).
(69) A. Ishihara, *Adv. Polym. Sci.*, **7**, 499 (1971).
(70) P. J. Flory, *Statistical Thermodynamics of Chain Molecules*, Interscience, New York, 1969.
(71) A. Yu. Grosberg and A. R. Khokhlov, *Statistical Physics of Macromolecules*, AIP Press, The American Institute of Physics, New York, 1994.
(72) P. J. Flory, *Proc. Roy. Soc., London Ser., A* **351**, 351 (1976).
(73) P. J. Flory, in *Contemporary Topics in Polymer Science*, E. M. Pearce and M. Schaefgen, Eds., Plenum, New York, 1977, Vol. 2.
(74) P. J. Flory, *Selected Works Vol. 3*, Stanford University Press, Stanford, Cal., 1985.
(75) H. R. Kricheldorf and J. Erxleben. *Polymer*, **31**, 944 (1990).
(76) H. R. Kricheldorf, G. Schwartz, A. Domschke, and V. Linzer, *Macromolecules*, **26**, 5161 (1994).
(77) H. R. Kricheldorf, V. Linzer, and Ch. Bruhn, *J. Macromol. Sci. Chem.*, **31**, 1315 (1994).
(78) H. R. Kricheldorf, V. Linzer, J. de Abajo, and J. de la Campa, *J. Macromol. Sci. Chem.*, **32**, 311 (1995).
(79) H. R. Kricheldorf and V. Linzer, *Polymer*, **36**, 1893 (1995).
(80) G. Figari and C. Coasta, *Macromol. Theory Simul.*, **6**, 29 (1996).
(81) W. Brostow and J. Sochanski, *J. Mater. Sci.*, **10**, 2134 (1975).
(82) E. Bianchi, E. Marsano, C. Costa, G. Conio, and S. Bisbano. *Macromol. Chem. Phys.*, **198**, 1239 (1997).
(83) M. Ballauff, D. Wu, P. J. Flory, and Ber. Bunsenges, *Phys. Chem.*, **88**, 524, 530 (1984).
(84) M. Ballauff, *Macromolecules*, **19**, 1366 (1986).
(85) M. Ballauff, *Mol. Cryst. Liq. Cryst. Lett.*, **4**, 15 (1986).
(86) S. Clan, U. Gallenkamp, M. Wolf, and J. H. Wendorff,

in *Integration of Fundamental Polymer Science and Technology*, P. Lemstra and L. A. Kleintjens, Eds., Elsevier Appl. Sci., London, 1990, Vol. IV.
(87) U. Gallenkamp, PhD thesis, TH Darmstadt, 1989.
(88) B. Schartel, V. Stuempflen, J. Wendling, J. H. Wendorff, W. Heitz, and R. Neuhaus, *Coll. Polym. Sci.*, **274**, 911 (1996).
(89) L. Stickfort, G. Poersch, and M. Hess, *J. Polym. Sci. A: Polym. Chem.*, **34**, 1325 (1996).
(90) R. Woelke and M. Hess, *Polym Eng. & Sci.*, **37** (1997) (accepted).
(91) J. Walasek and M. Hess, Work in progress.
(92) W. Brostow, K. Hibner, and J. Walasek, to be published: private communication J. Walasek.
(93) A. Ziabicki and J. Walasek, *Macromolecules*, **11**, 471 (1978).
(94) J. Walasek and A. Ziabicki, *Coll. Polym. Sci.*, **226**, 114 (1988).
(95) J. K. Moscicki, *Vth International Conference on Polymer Characterization*, Denton, TX, U. S. A., Book of Abstracts I-06 (1997); to be published in *Polym Eng. Sci.*, **37** (1997).